

UNIVERSITÉ DU QUÉBEC À RIMOUSKI

**VARIABILITÉ SPATIALE ET TEMPORELLE DU
COEFFICIENT D'ABSORPTION DE LA LUMIÈRE PAR LE
PHYTOPLANCTON DES MERS ARCTIQUES
CANADIENNES**

Mémoire présenté
dans le cadre du programme de maîtrise en océanographie
en vue de l'obtention du grade de maître ès sciences

PAR
© Corinne Bourgault Brunelle

Avril 2012

UNIVERSITÉ DU QUÉBEC À RIMOUSKI
Service de la bibliothèque

Avertissement

La diffusion de ce mémoire ou de cette thèse se fait dans le respect des droits de son auteur, qui a signé le formulaire « *Autorisation de reproduire et de diffuser un rapport, un mémoire ou une thèse* ». En signant ce formulaire, l'auteur concède à l'Université du Québec à Rimouski une licence non exclusive d'utilisation et de publication de la totalité ou d'une partie importante de son travail de recherche pour des fins pédagogiques et non commerciales. Plus précisément, l'auteur autorise l'Université du Québec à Rimouski à reproduire, diffuser, prêter, distribuer ou vendre des copies de son travail de recherche à des fins non commerciales sur quelque support que ce soit, y compris l'Internet. Cette licence et cette autorisation n'entraînent pas une renonciation de la part de l'auteur à ses droits moraux ni à ses droits de propriété intellectuelle. Sauf entente contraire, l'auteur conserve la liberté de diffuser et de commercialiser ou non ce travail dont il possède un exemplaire.

Composition du jury :

Prof. Suzanne Roy, présidente du jury, ISMER-UQAR

Dr Pierre Larouche, directeur de recherche, Institut Maurice-Lamontagne

Prof. Michel Gosselin, codirecteur de recherche, ISMER-UQAR

Dr Emmanuel Devred, membre externe, Institut océanographique de Bedford

Dépôt initial le 17 mai 2011

Dépôt final le 27 avril 2012

AVANT-PROPOS

Ce mémoire de maîtrise traite de la variabilité spatiale du coefficient d'absorption de la lumière par le phytoplancton des mers arctiques dans le détroit et la baie d'Hudson, la baie de Baffin, l'archipel arctique canadien et le golfe d'Amundsen. Il traite également de la variabilité de ce coefficient dans le golfe d'Amundsen au cours de trois saisons (i.e. à l'automne 2007, au printemps 2008 et à l'été 2008). Cette étude vise l'amélioration des connaissances sur les propriétés optiques inhérentes de l'eau de mer et le développement de modèles bio-optiques appropriés pour les milieux polaires. Ce mémoire est une contribution aux programmes canadiens de recherche Étude du chenal de séparation circumpolaire / Circumpolar Flaw Lead (CFL) system study et ArcticNet, un réseau de centres d'excellence du Canada (RCE).

Ce mémoire se compose d'un résumé et d'une introduction générale en français, d'un chapitre central rédigé sous forme d'article scientifique en anglais et d'une conclusion générale en français. Cet article a été soumis et accepté au *Journal of Geophysical Research – Oceans*, édition spéciale de CFL. Les résultats de ce travail ont été présentés à plusieurs rencontres scientifiques sous forme d'affiche (en 2008 : *Ocean Optics Conference*, Accra, Italy, *Assemblée générale annuelle de Québec-Océan*, Rivière-du-Loup et *Arctic Change Conference*, Québec; en 2009 : *Assemblée générale annuelle de Québec-Océan*, Rimouski, *CFL All-Hands Meeting*, Winnipeg et au colloque de vulgarisation scientifique *La biologie dans tous ses états* des étudiants aux cycles supérieurs de l'Université du Québec à Rimouski (UQAR), Rimouski.

Je tiens à remercier les professeurs Suzanne Roy (ISMER-UQAR) pour son aide précieuse lors de l'analyse des pigments, Huixiang Xie (ISMER-UQAR) pour m'avoir permis d'analyser les données concernant l'absorption de la lumière par la matière dissoute et colorée dans le golfe d'Amundsen (projet CFL) et Yves Gratton (INRS-ETE) pour m'avoir fourni les profils de température et de salinité de la colonne d'eau. Un remerciement spécial aux officiers et à l'équipage du navire de recherche NGCC Amundsen pour leur soutien logistique et technique lors des missions dans l'Arctique canadien, à Sélima Ben Mustapha pour l'échantillonnage lors de la mission ArcticNet 2007, à Eva Alou pour les analyses pigmentaires, à Mathieu Ardyna, Benoît Philippe et Joannie Ferland pour la collecte des échantillons et l'analyse fluorométrique de la chlorophylle *a* ainsi qu'à Christopher-John Mundy et Luc Bourgeois pour le calcul et l'interprétation du coefficient d'absorption de la lumière par le phytoplancton.

Cette étude a été financée par le programme de l'Année polaire internationale du Gouvernement du Canada, le Conseil de recherches en sciences naturelles et en génie du Canada (CRSNG) et le réseau des centres d'excellence (RCE) ArcticNet. Je remercie les membres du jury pour leur support, l'Institut des sciences de la mer de Rimouski et surtout, mes directeurs de recherche pour les bourses d'études qu'ils m'ont attribuées durant ma maîtrise ainsi que le Programme de formation scientifique dans le Nord du ministère des Affaires indiennes et du Nord pour son appui financier lors du travail en mer.

RÉSUMÉ

Les spectres d'absorption de la lumière par le phytoplancton ($a_\phi(\lambda)$) des mers arctiques ont été mesurés dans les eaux du détroit et de la baie d'Hudson, de la baie de Baffin, de l'archipel canadien et du golfe d'Amundsen. Les algues, principalement dominées par le picophytoplancton (< 5 µm), n'était pas la composante principale des eaux arctiques tandis que la matière organique colorée et dissoute (CDOM) représentait près de 70% du bilan total d'absorption de la lumière. À l'automne, les faibles valeurs d'absorption spécifique par le phytoplancton ($a_\phi^*(443) = a_\phi(443)/T\text{Chl } a$) ont été expliquées par les processus d'acclimatation observés dans les milieux limités en lumière et/ou en nutriments. Cette limitation et la présence importante de CDOM (absorbant fortement les ultraviolets) semblent favoriser la croissance du phytoplancton ayant des pigments accessoires qui absorbent la lumière à de plus grandes longueurs d'onde. Le ratio des caroténoïdes photoprotecteurs et photosynthétiques (PPC:PSC), inversement proportionnel à la salinité et la taille des cellules, décroît vers le Haut-Arctique canadien. Les valeurs de $a_\phi^*(443)$ les plus élevées furent observées dans les eaux du golfe d'Amundsen de mai à juin 2008 (printemps/été) et dans le système de la baie d'Hudson de septembre à octobre 2005 (automne), régions spatio-temporelles relativement moins limitées en lumière et/ou en nutriments. Ces résultats permettront éventuellement d'améliorer les modèles bio-optiques de télédétection dans le but de suivre de façon plus efficace les changements imminents de l'océan Arctique.

Mots-clés: absorption, phytoplancton, pigments, mers arctiques, photoacclimatation

ABSTRACT

Phytoplankton light absorption spectra ($a_\phi(\lambda)$) were measured in the Canadian Arctic (i.e. the Amundsen Gulf, Canadian Arctic Archipelago, northern Baffin Bay and Hudson Bay system) to improve algorithms used in remote-sensing models of primary production. The algae, mostly dominated by picophytoplankton ($< 5 \mu\text{m}$), was not the major light absorption factor in the four provinces; the colored dissolved organic matter (CDOM) contributing up to 70% of total light budget. During the fall, the low total chlorophyll *a*-specific $a_\phi^*(443)$ ($a_\phi(443)/\text{TChl } a$) coefficients of the Canadian High Arctic were associated to acclimation processes occurring in light- and/or nutrients-limited environments. Those limitations and high proportion of CDOM (absorbing strongly the ultraviolet) seem to allow the growth of phytoplankton with accessory pigments absorbing light at longer wavelengths. The ratio of photoprotective and photosynthetic carotenoids (PPC:PSC), inversely proportional to the salinity and the cell size, decreases throughout the Canadian High Arctic. The highest $a_\phi^*(443)$ values were observed in the Amundsen Gulf from May to July (i.e. spring/summer) as well as in the Hudson Bay system from September to October (i.e. fall), spatio-temporal regions relatively less limited by light and/or nutrients availability. These results will ultimately allow the accurate monitoring of phytoplankton biomass and productivity evolution that is likely to take place as a result of the fast-changing Arctic environment.

Keywords: light absorption, phytoplankton, algal pigments, arctic seas, photoacclimation

TABLE DES MATIÈRES

AVANT-PROPOS	VII
RÉSUMÉ.....	IX
ABSTRACT	XI
TABLE DES MATIÈRES	XIII
LISTE DES TABLEAUX.....	XV
LISTE DES FIGURES.....	XVII
1. INTRODUCTION GÉNÉRALE.....	19
1.1. LA PROBLÉMATIQUE	19
1.2. LES OBJECTIFS DE L'ÉTUDE	23
1.3. LES CONCEPTS FONDAMENTAUX.....	24
2. VARIABILITY OF PHYTOPLANKTON LIGHT ABSORPTION IN CANADIAN ARCTIC SEAS.....	27
2.1 INTRODUCTION.....	28
2.2 MATERIALS AND METHODS	30
2.2.1 Data Sampling.....	30
2.2.2. Pigment composition and taxonomy.....	31
2.2.3. Phytoplankton size structure.....	32
2.2.4. Particulate and algal absorption measurements	33
2.2.5. Colored dissolved organic matter (CDOM) absorption measurements	34
2.2.6. Data processing and statistical analyses.....	34

2.3 RESULTS AND DISCUSSION	38
2.3.1. Absorption Budget.....	38
2.3.2. Regional variability.....	42
2.3.3. Vertical variability.....	50
2.3.4. Seasonality	56
2.4. CONCLUSION.....	57
3. CONCLUSION	59
4. RÉFÉRENCES BIBLIOGRAPHIQUES.....	60

LISTE DES TABLEAUX

Table 1. Symbols and abbreviations	37
Table 2. Phytoplankton (a_ϕ), non algal material (a_{na}) and colored dissolved organic matter (a_{cdom}) absorption coefficients at 443 nm, their relative contributions to the total nonwater absorption (a_{t-w}) and chlorophyll α concentration measured by fluorometry ($\text{Chl } \alpha^{\text{Fluo}}$) in surface waters ($Z \leq Z_{50\%}$) of the four oceanographic provinces. Average, SD (in parentheses) and range are shown; n = number of observations.....	41
Table 3. Constants for the power law regression $a_\phi(443) = A_\phi(443)[\text{TChl } \alpha]^{B\phi(443)}$ at 443 nm for surface ($Z \leq Z_{50\%}$) and deeper waters ($Z > Z_{50\%}$). Regressions including all depths are shown where r^2 is the coefficient of determination, n is the number of observations. Range, mean and SD of TChl α used for the regression are presented for each province. No regression has been calculated for the Canadian Arctic Archipelago; the range of TChl α in surface waters was too short.....	55

LISTE DES FIGURES

Figure a. Schéma explicatif de la variation du coefficient spécifique d'absorption de la lumière par le phytoplancton $a_\phi^*(\lambda)$ et de l'effet d'empilement des pigments dans la cellule en fonction des variations de la taille des cellules et des variations saisonnières.....	xxviii
Figure 1. Location of sampling stations in the Canadian High Arctic and Hudson Bay system during: * fall 2005, • fall 2007 and ○ spring/summer 2008. The Canadian High Arctic is divided in three provinces: Amundsen Gulf, Canadian Arctic Archipelago (stns 301, 302, 308, 309, 310, 2010) and northern Baffin Bay (stns 101, 108, 111, 115, 134).	31
Figure 2. Relative contributions of phytoplankton (a_ϕ), non algal matter (a_{na}) and colored dissolved organic matter (a_{cdom}) to total non-water absorption at five SeaWiFS wavelengths in the four oceanographic provinces (all depths). Full grey lines = a_{cdom} , horizontal dashed lines = a_ϕ and diagonal dashed lines = a_{na}	39
Figure 3. Box plots of the total Chl α -specific light absorption by phytoplankton ($a_\phi^*(\lambda)$) of each oceanographic province at eight SeaWiFS wavelengths. Descriptive statistics were calculated for all depths, except in the Hudson Bay system where only surface waters had been sampled. Spectra averages, between 400 and 700 nm, are shown at the surface for $Z \leq Z_{50}$ (i.e. > 50% of surface irradiance) and deeper waters for $Z > Z_{50}$ (i.e. from 50% to 1% of surface irradiance).	43
Figure 4. Variations of (a) the absorption coefficient of phytoplankton $a_\phi(443)$ as a function of the absorption coefficient of phytoplankton $a_\phi(676)$ and (b) the ratio of $a_\phi(443)$ to $a_\phi(676)$ as a function of the total Chl α concentrations for all depths, shown	

in log scale. Dashed lines of figures (a) and (b) represent the regression lines of <i>Babin et al.</i> [2003]. The (c) $a_\phi(443)$ coefficient as a function of the total Chl <i>a</i> concentrations at the surface (i.e. > 50% of surface irradiance) and (d) deeper waters (i.e. from 50% to 1% of surface irradiance) are shown. In (c) and (d), regression lines of <i>Wang et al.</i> [2005] for the Beaufort and Chukchi seas, <i>Matsuoka et al.</i> [2007] for the western Arctic Ocean and <i>Bricaud et al.</i> [2004] for the World Oceans are drawn for comparison. Note that the absorption coefficient was measured at 440 nm for surface waters in <i>Bricaud et al.</i> [2004], and for all depths in <i>Matsuoka et al.</i> [2007] and <i>Wang et al.</i> [2005].	46
Figure 5. Spatial variations of the (a) total Chl <i>a</i> -specific phytoplankton light absorption coefficient $a_\phi^*(443)$, (b) blue-to-red ratio $a_\phi(443):a_\phi(675)$, (c) relative proportion of picophytoplankton, (d) ratio of photoprotective carotenoids (PPC) and photosynthetic carotenoids (PSC), (e) ratio of Chl <i>b</i> and TChl <i>c</i> and (f) salinity in surface waters (i.e. > 50% of surface irradiance) of the Canadian Arctic during fall.....	49
Figure 6. Relationships between total Chl <i>a</i> concentration and (a) total accessory pigments (AccP), the regression of our study corresponds to: $\text{AccP} = 0.813(\text{TChl } a)^{0.954}$ ($r^2 = 0.92$), (b) photoprotective carotenoids (PPC), (c) <i>Package effect</i> index $Q^*(675)$ and (d) total Chl <i>a</i> -specific photosynthetic carotenoids ($\text{PSC}^* = \text{PSC}/\text{TChl } a$) in the four oceanographic provinces. Dashed lines represent in (a) regression and (b) approximated range measured by <i>Babin et al.</i> [2003]. Grey boxes represent the <i>Bricaud et al.</i> [2004]'s observation in North Atlantic waters dominated by small cells (February to May).	52
Figure 7. Relative contribution of the main marker pigments to total pigment concentration (weight-to-weight) in the (a) northern Baffin Bay, (b) Canadian Arctic Archipelago, (c) Amundsen Gulf and (d) Hudson Bay system for surface ($Z \leq Z_{50\%}$) and deeper waters ($Z > Z_{50\%}$) of the euphotic zone during fall. See Table 1 for pigment abbreviations.....	54

1. INTRODUCTION GÉNÉRALE

1.1. LA PROBLÉMATIQUE

L'océan Arctique connaît actuellement une accélération du déclin du couvert de glace de mer (Barber & Hanesiak 2004, Barber *et al.* 2008, Comiso *et al.* 2008) offrant ainsi un tout nouvel environnement pour la croissance du phytoplancton (Arrigo *et al.* 2008). Cette région étant difficile d'accès, la télédétection semble être un moyen efficace pour d'observer dans l'avenir les effets de la fonte du couvert de glace sur l'écosystème marin. Des algorithmes empiriques et semi-analytiques relient à ce jour la couleur des eaux à la biomasse algale (O'Reilly *et al.* 1998, 2000, Antoine & Morel 1999). Cependant, ces algorithmes ont été développés utilisant principalement des données des mers tempérées et ont montré certaines difficultés à représenter la réalité des milieux polaires (Dierssen & Smith, 2000, Reynolds *et al.* 2001, Stramska & Stramski 2003, Wang & Cota 2003). Ceci est particulièrement vrai dans les eaux côtières arctiques et subarctiques du Canada qui contiennent des concentrations élevées de matière organique dissoute et colorée (CDOM) (Pegau 2002, Bélanger *et al.* 2006, Granskog *et al.* 2007, Matsuoka *et al.* 2007, 2009, 2011, Retamal *et al.* 2007). Cette matière jaune-brun provoque une surestimation de la concentration de chlorophylle *a* (Chl *a*) utilisant les algorithmes opérationnels existants. Ainsi, des algorithmes régionaux et adaptés ont été proposés pour améliorer les calculs de la concentration de Chl *a* dans les eaux de surface des mers arctiques (Wang & Cota 2003, Cota *et al.* 2004).

Intrinsèquement, ces algorithmes reposent sur la connaissance des propriétés optiques inhérentes des eaux : l'absorption et la diffusion de la lumière par les particules en suspension et par la matière organique dissoute. En particulier, les spectres d'absorption de la lumière par le phytoplancton ($a_\phi(\lambda)$) changent en fonction des différentes communautés

phytoplanctoniques (Hoepffner & Sathyendranath 1992, Babin *et al.* 1993, Lutz *et al.* 2003, Sathyendranath *et al.* 2004, Devred *et al.* 2005, Retamal *et al.* 2008). Ces espèces peuvent également s'adapter aux différentes intensités lumineuses ambiantes en modifiant leur contenu cellulaire soit en fonction des pigments et/ou des centres réactionnels de la photosynthèse (Falkowski & Raven 2007). Pour des intensités lumineuses faibles, ces espèces peuvent augmenter la concentration de pigments par cellule et changer l'organisation des photosystèmes (Falkowski & Owens 1980). Ainsi, l'efficacité de l'absorption de la lumière décroît au fur et à mesure que la concentration de pigments par cellule augmente. Ce phénomène, caractérisé par l'*effet d'empilement* des pigments (Falkowski *et al.* 1985, Morel & Ahn 1990), croit généralement avec la taille et la concentration des algues de sorte que le coefficient spécifique d'absorption $a_{\phi}^*(443)$ ($a_{\phi}(443)/\text{Chl } a$, $\text{m}^2 \text{ mg Chl } a^{-1}$) soit une fonction non linéaire de la concentration de Chl *a* (Morel & Bricaud 1981, Morel 1991).

De ce fait, la variabilité des spectres $a_{\phi}^*(\lambda)$ entre 400 nm et 700 nm est en grande partie expliquée par la taille et la composition pigmentaire du groupe phytoplanctonique dominant (Ciotti *et al.* 2002, Bricaud *et al.* 2004, Roy *et al.* 2008). Cependant, de petites cellules adaptées à de faibles intensités lumineuses pourraient également être caractérisées par l'*effet d'empilement* des pigments dans la cellule (Morel 1991). Dans l'océan Arctique et ses mers adjacentes, de très petites espèces endémiques de picoprasinophytes (Lovejoy *et al.* 2007, Tremblay *et al.* 2009) et adaptées à de faibles intensités lumineuses pourraient donc être caractérisées par de faibles coefficients $a_{\phi}^*(\lambda)$ (Matsuoka *et al.* 2007, 2009, 2011, Wang *et al.* 2005). Il semble alors être essentiel d'améliorer nos connaissances de la variabilité saisonnière et régionale du coefficient $a_{\phi}^*(\lambda)$ utilisé dans les algorithmes de télédétection et les modèles bio-optiques de production primaire (Sathyendranath *et al.* 2001, 2004, Devred *et al.* 2006, Pabi *et al.* 2008, Arrigo *et al.* 2011) en Arctique.

Finalement, les propriétés physiques de la colonne d'eau et la disponibilité en nutriments influencent la répartition et la taille du phytoplancton en Arctique. Ceci cause en grande partie la variabilité des propriétés d'absorption de la lumière selon les régions. Le Haut-Arctique canadien est divisé en trois régions de propriétés physiques, chimiques et biologiques différentes : (1) la mer de Beaufort comprenant le plateau du Mackenzie et le golfe d'Amundsen, (2) l'archipel arctique canadien et (3) la baie de Baffin. Dans la partie nord de la baie de Baffin se trouve l'une des plus grande polynie de l'Arctique, la polynie des eaux du Nord (Ingram *et al.* 2002). Cette polynie récurrente se crée par la formation d'embâcles de glaces au nord et un fort écoulement vers le sud (Melling *et al.* 2001, Ingram *et al.* 2002). Le courant groenlandais transporte par ailleurs une masse d'eau plus chaude et plus salée provenant du sud-est (masse d'eau de l'Atlantique) créant des conditions physiques et biologiques différentes dans l'axe ouest-est du nord de la baie de Baffin (Melling *et al.* 2001, Ingram *et al.* 2002). Lors de la prolifération printanière du phytoplancton, c'est le long de la côte du Groenland que l'on retrouve une majorité de diatomées comparativement aux eaux plus froides le long de la côte canadienne contenant davantage de flagellées (Vidussi *et al.* 2004). L'amplitude et la durée de la prolifération des algues dans cette région seraient relativement importantes et contrôlées par l'apport d'éléments nutritifs dans la zone euphotique induit par le vent (Tremblay *et al.* 2002).

À la fin de l'été, la taille des cellules entre 2 et 10 µm tend à augmenter dans la baie de Baffin relativement aux autres régions du Haut-Arctique canadien (Tremblay *et al.* 2009). D'après la même étude, le picophytoplancton (< 2 µm) serait plus abondant dans le passage du nord-ouest et composé d'eucaryote (i.e. prasinophyceae *micromonas*). Ce passage, situé dans l'archipel canadien, relie la baie de Baffin et la mer de Beaufort créant ainsi un réseau complexe des caractéristiques biogéographiques. Le couvert de glace dans cette région participe également au contrôle des processus biologiques et au piégeage du dioxyde de carbone; les algues de glace étant pratiquement broutées au fur et à mesure lorsqu'elles se détachent du couvert de glace peuvent par ailleurs être exportées rapidement vers le fond lors de la fonte printanière (Fortier *et al.* 2002).

Les variations saisonnières extrêmes du couvert de glace, de la température, de lumière, de turbidité et des courants s’observent également dans le golfe d’Amundsen, au sud-est de la mer de Beaufort, incluant la polynie du Cape Bathurst. Lors de la fonte du couvert de glace du plateau du Mackenzie, les eaux douces et turbides du fleuve Mackenzie se propagent en partie vers le golfe d’Amundsen accentuant ainsi la stratification déjà causée par l’eau douce des glaces fondues (Carmack *et al.* 2004). La production primaire de la baie de Franklin (golfe d’Amundsen) ainsi que de l’océan Arctique en général, serait également davantage influencée par la disponibilité en nutriments et des apports d’eau douce que par le changement d’intensité lumineuse en période d’eau libre (Tremblay *et al.* 2008).

Dans le Bas-Arctique canadien, le système de la baie d’Hudson se sépare de la même façon en trois régions : (1) la baie d’Hudson, (2) le détroit d’Hudson et (3) le bassin de Foxe. La baie d’Hudson, grandement influencée par les apports d’eau douce des rivières près des côtes, est partiellement couverte de glace durant l’hiver et est caractérisée par une très grande variabilité des propriétés optiques inhérentes ainsi que des paramètres biologiques comparativement au détroit d’Hudson et au bassin de Foxe (Granskog *et al.* 2007, Lapoussière *et al.* 2009). Ainsi, cette vaste zone d’étude peut induire une variabilité spatiale considérable du coefficient d’absorption de la lumière par le phytoplancton des mers arctiques.

1.2. LES OBJECTIFS DE L'ÉTUDE

Les objectifs de cette étude sont : (1) de répertorier la variabilité spatio-temporelle des spectres d'absorption de la lumière par le phytoplancton du Haut- et Bas-Arctique canadien entre les différentes périodes d'éclairement et (2) de comparer la variabilité du coefficient d'absorption $a_\phi^*(\lambda)$ selon les paramètres biologiques (i.e. taille des cellules et pigments) et physiques (stratification des eaux, absorption particulaire ($a_{\text{na}}(\lambda)$) et dissoute ($a_{\text{cdom}}(\lambda)$) de la matière) disponibles. L'hypothèse de travail est que les variations saisonnières extrêmes d'éclairement et des propriétés biogéochimiques, ainsi que la présence d'espèces endémiques et adaptées dans cette grande zone d'étude, influencerait de façon significative les propriétés d'absorption de la lumière par le phytoplancton en fonction des régions et des saisons.

Pour ce faire, les données de cette étude, collectées à bord du brise glace canadien NGCC Amundsen dans le cadre du programme canadien de recherche ArcticNet, ont été collectées dans la baie d'Hudson, le nord de la baie de Baffin, l'archipel arctique canadien et le golfe d'Amundsen permettant ainsi de comparer les diverses régions à l'automne 2007. De plus, le programme de recherche Circumpolar Flaw Lead (CFL) a permis d'échantillonner les eaux du golfe d'Amundsen au printemps et à l'été 2008 dans le cadre du programme canadien de l'année polaire internationale permettant d'observer les variabilités saisonnières de cette région. Plusieurs profondeurs de la zone euphotique ont été échantillonnées incluant les maximums de chlorophylle sous la surface afin de vérifier si différentes intensités lumineuses et disponibilités en nutriments modifiaient les propriétés d'absorption de communautés phytoplanctoniques distinctes. Par contre, seulement les eaux de surface ont été échantillonnées dans le système de la baie d'Hudson.

1.3. LES CONCEPTS FONDAMENTAUX

Les facteurs déterminants du coefficient $a_\phi(\lambda)$ sont la taille des cellules, leur forme et leur composition pigmentaire (Kirk 1984). Il est possible de diviser en deux grandes classes les groupes phytoplanctoniques d'un point de vue optique soit; le groupe des prasinophyceae et chlorophycea (pigments de Chl *b* + MgDVP + prasinoxanthin + néoxanthin + violaxanthin) et ensuite le groupe des bacillariophyta, dinophyta, prymnesiophycea et chrysophycea (pigments de TChl *c* + fucoxanthin + diadinoxanthin) (Jeffrey *et al.* 1997, Vidussi *et al.* 2004). Ces deux groupes représentent en fait les algues vertes (contenant la Chl *b*) et les algues brunes (contenant la Chl *c*). Ces deux catégories sont également reliées respectivement aux petites cellules, caractérisées par les caroténoïdes photoprotectrices (PPC), et aux grandes cellules, caractérisées par les caroténoïdes photosynthétiques (PSC) (Uitz *et al.* 2006, Moreno *et al.* 2012).

La figure *a* illustre que les cellules de petites tailles, provenant des milieux oligotrophes, sont naturellement caractérisées par des coefficients $a_\phi^*(\lambda)$ élevés. Dans les milieux eutrophes, les cellules de plus grandes tailles sont caractérisées par des coefficients $a_\phi^*(\lambda)$ faibles causés par l'*effet d'empilement* des pigments dans la cellule. D'un point de vue saisonnier, les espèces phytoplanctoniques peuvent s'adapter aux diminutions de l'éclairement et de la disponibilité en nutriments au cours de la saison en eaux libres. Pour ce faire, le nombre de pigment par cellules augmente de même que l'*effet d'empilement* diminuant ainsi les coefficients $a_\phi^*(\lambda)$. La figure *a* montre qu'une biomasse élevée au printemps non limitée en lumière et en nutriments possède des coefficients $a_\phi^*(\lambda)$ élevés. À l'automne, les facteurs limitant la croissance du phytoplancton entraîneraient également une diminution du coefficient $a_\phi^*(\lambda)$. Les communautés phytoplanctoniques peuvent donc s'adapter aux milieux de faibles intensités lumineuses, si les apports en nutriments sont insuffisants (Dubinsky & Stambler 2009). Il a été observé que les proportions de xanthophylles peuvent également être plus faibles si le cycle des xanthophylles, moyen rapide de photoacclimatation (Demers *et al.* 1991), est moins actif (Kashino *et al.* 2002).

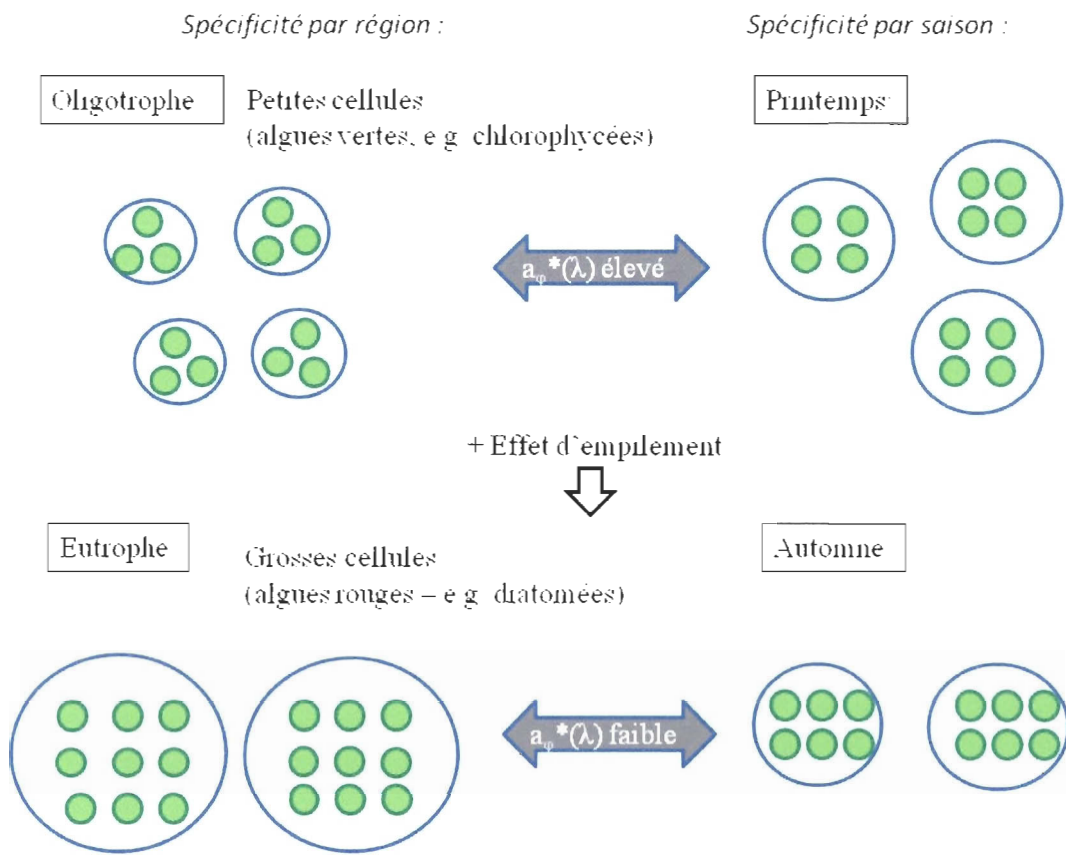


Figure a. Schéma explicatif de la variation du coefficient spécifique d'absorption de la lumière par le phytoplancton $a_{\phi}^*(\lambda)$ et de l'effet d'empilement des pigments dans la cellule en fonction des variations de la taille des cellules et des variations saisonnières.

2. VARIABILITY OF PHYTOPLANKTON LIGHT ABSORPTION IN CANADIAN ARCTIC SEAS

2.1 INTRODUCTION

The Arctic Ocean is currently experiencing significant changes caused by the sea-ice cover decline [Barber and Hanesiak, 2004; Barber *et al.*, 2008; Comiso *et al.*, 2008] opening a whole new environment for phytoplankton growth [Arrigo *et al.*, 2008]. Considering the difficulty to access the region, remote sensing is probably the best method to monitor the effects of ice cover decrease on the marine ecosystem. Empirical and semi-analytic algorithms already exist to link remote sensing reflectance to phytoplankton biomass [O'Reilly *et al.*, 1998, 2000; Antoine and Morel, 1999]. These algorithms have, however, been developed mostly using non polar open ocean data and have been shown to be biased for polar waters [Dierssen and Smith, 2000; Reynolds *et al.*, 2001; Stramska and Stramski, 2003; Wang and Cota, 2003]. This is particularly true in the coastal waters of the Canadian Arctic and Subarctic as those waters contain high concentrations of colored dissolved organic matter (CDOM) [Pegau, 2002; Bélanger *et al.*, 2006; Granskog *et al.*, 2007; Matsuoka *et al.*, 2007, 2009, 2011; Retamal *et al.*, 2007] leading to an overestimation of the chlorophyll a (Chl *a*) concentrations using current operational algorithms. Regionally adapted algorithms have been proposed for the Arctic to improve the retrieval of the Chl *a* concentration [Wang and Cota, 2003; Cota *et al.*, 2004].

Light reflectance from the sea is a function of the absorption and scattering of particles and dissolved matter. In particular, the phytoplankton light absorption spectra ($a_\phi(\lambda)$) changes with different phytoplankton communities [Hoepffner and Sathyendranath, 1992; Babin *et al.*, 1993; Lutz *et al.*, 2003; Sathyendranath *et al.*, 2004; Devred *et al.*, 2005; Retamal *et al.*, 2008]. The determinant factors of the $a_\phi(\lambda)$ variability are the pigments and the cell sizes [Kirk, 1994]. Phytoplankton species can adapt to variable irradiance by altering their cellular content in light-harvesting pigments and/or reaction centers [Falkowski and Raven, 2007]. When exposed to low light, phytoplankton usually increases their pigment concentration and changes the organization of these pigments within their photosynthetic units [Falkowski and Owens, 1980]. The efficiency of light absorption

decreases as the pigment concentration per cell increases. This phenomenon, the *package effect* [Falkowski *et al.*, 1985; Morel and Ahn, 1990], generally increases with cell size and phytoplankton concentration making the Chl *a*-specific phytoplankton light absorption coefficient $a_{\phi}^*(443)$ ($a_{\phi}(443)/\text{Chl } a, \text{ m}^2 \text{ mg Chl } a^{-1}$) a nonlinear function of Chl *a* concentration [Morel and Bricaud, 1981; Morel, 1991].

Nowadays, most of the natural variability in the spectral shape of $a_{\phi}^*(\lambda)$ between 400 and 700 nm can be explained by the dominant phytoplankton group and cell size [Ciotti *et al.*, 2002; Bricaud *et al.*, 2004; Roy *et al.*, 2008]. However, small phytoplankton cells photoadapted to low light could experience an important *package effect* [Morel, 1991]. In the Arctic Ocean and adjacent seas, endemic picoprasinophytes adapted to low light [Lovejoy *et al.*, 2007; Tremblay *et al.*, 2009] and weak nutrients supply [Dubinsky and Stambler, 2009] could consequently have weak $a_{\phi}^*(\lambda)$ values [Matsuoka *et al.*, 2007, 2009, 2011; Wang *et al.*, 2005]. It thus appears essential to improve the knowledge of the seasonal and regional variations of $a_{\phi}^*(\lambda)$ for the development of ocean color remote sensing algorithms and phytoplankton light absorption models that will provide an accurate estimation of primary production in the Arctic [Sathyendranath *et al.*, 2001, 2004; Devred *et al.*, 2006; Pabi *et al.*, 2008; Arrigo *et al.*, 2011].

The objectives of this study are 1) to determine the main variability sources of $a_{\phi}^*(\lambda)$ and 2) characterize spatial and temporal variations of phytoplankton absorption spectra, including the light budget, in the different oceanographic provinces of the Canadian Arctic. A large dataset of absorption spectra has been gathered and analyzed regarding available physical (i.e. water stratification, absorption by non algal material (a_{na}) and colored dissolved organic matter (a_{cdom})) and biological (i.e. cell sizes and algal pigments) parameters. Our hypotheses are that 1) spatial variability in phytoplankton light absorption spectra is explained by differences in phytoplankton cell size and water column stratification and 2) the low of $a_{\phi}^*(\lambda)$ values is related to the decrease of solar elevation and incident irradiance.

2.2 MATERIALS AND METHODS

2.2.1 Data Sampling

Sampling was conducted in the Hudson Bay system from 22 September to 13 October 2005 and in northern Baffin Bay, Canadian Arctic Archipelago and in the Amundsen Gulf from 19 October to 15 November 2007, onboard the icebreaker CCGS *Amundsen* as part of the Canadian research program ArcticNet (Figure 1). Those three aforementioned oceanographic provinces are identified as the Canadian High Arctic. Additional data were obtained in the Amundsen Gulf from 8 May to 6 July 2008 during the International Polar Year-Circumpolar-Flaw Lead system study (IPY-CFL).

In the present study, spring/summer and fall are defined as the time period between 8 May and 6 July and between 22 September and 15 November, respectively. At each station, the depth of the euphotic zone was determined with a Secchi disk and vertical profiles of temperature ($^{\circ}\text{C}$), salinity (psu) and *in vivo* fluorescence were performed using a Sea-Bird 911 *plus* CTD probe equipped with a SeaPoint chlorophyll fluorometer. Water samples were collected with 12 L Niskin-type bottles (OceanTest Equipment) at three optical depths (50%, 10% and 1% of surface irradiance), at depth of the subsurface chlorophyll fluorescence maximum (SCM) and at 60 m. In addition, surface samples (100% surface irradiance) were also collected using a clean bucket. This strategy was used for all cruises except for Hudson Bay system where samples were only taken at the surface. The vertical light attenuation coefficient (k in m^{-1}) was calculated using the formulation of *Holmes* [1970] expressed as $k = 1.44/Z_{\text{SD}}$, where Z_{SD} is the Secchi disk depth.

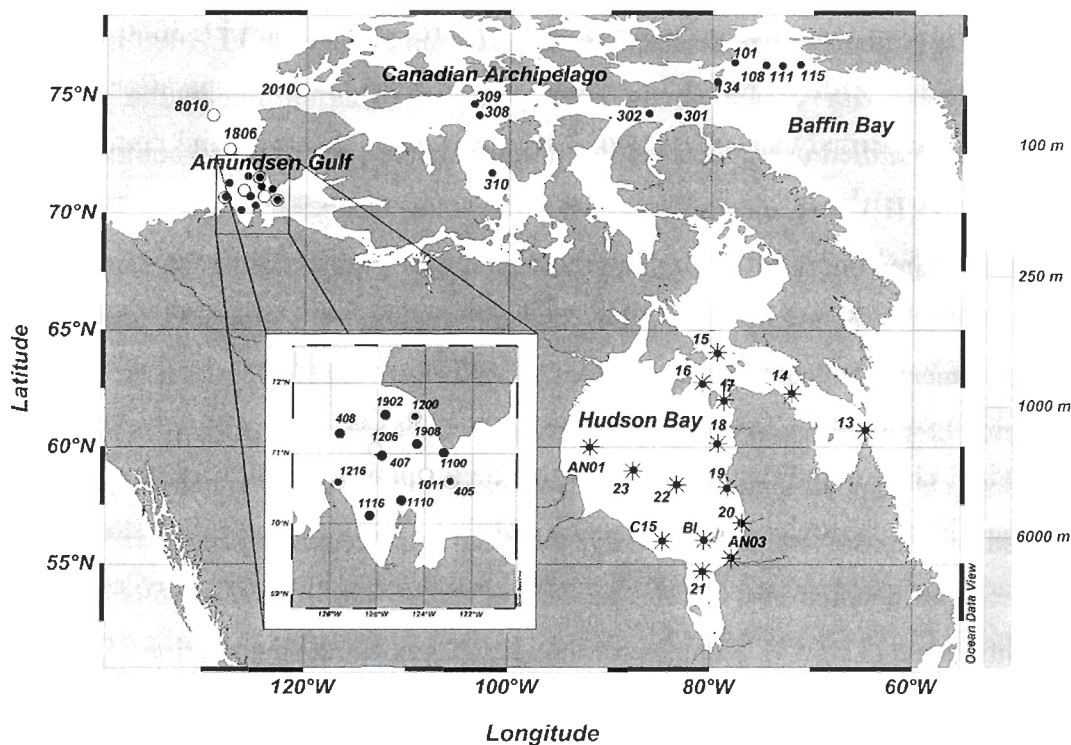


Figure 1. Location of sampling stations in the Canadian High Arctic and Hudson Bay system during: * fall 2005, • fall 2007 and ○ spring/summer 2008. The Canadian High Arctic is divided in three provinces: Amundsen Gulf, Canadian Arctic Archipelago (stns 301, 302, 308, 309, 310, 2010) and northern Baffin Bay (stns 101, 108, 111, 115, 134).

2.2.2. Pigment composition and taxonomy

Samples (1.5 to 2.0 L) for pigment composition were filtered onto 25 mm Whatman GF/F glass-fiber filters (nominal porosity of 0.7 µm), stored in cryovials and frozen in liquid nitrogen until measurement by reverse-phase high-performance liquid chromatography. Pigments were extracted from the filter in ice-cold 95% methanol using a sonicator (Ultrasonic Processor XL 2010). The extracts were cleared from the filter by centrifugation and further filtered on a 0.22 µm PTFE syringe filter. A 50 µL extract was then injected in a reversed phase C8 Waters Symmetry column (150 x 4.6 mm, 3.5 µm). Gradient elution was controlled by a Thermo Separation P4000 pump. The gradient elution

method used was developed by *Zapata and Garrido* [2000] (mobile phases A and B1, flow rate 1 ml min^{-1}). Pigments were detected using a Thermo Separation FL 3000 fluorescence detector in series with a photodiode array detector (Thermo Separation UV-6000). Pigments were identified using their retention time, visible spectrum and comparison with standards from DHI Water and Environment (Hørsholm, Denmark). This method allowed us to determine the concentrations of the most abundant pigments in each sample with a detection limit of 0.03 mg m^{-3} for Chl *a*. The distribution of major and taxonomically significant pigments in algal divisions/classes of *Jeffrey et al.* [1997] was used to describe phytoplankton communities. As already observed in the Canadian Arctic [*Tremblay et al.*, 2009], divinyl chlorophyll *a* and *b* (i.e. the two major pigments of *Prochlorococcus*) were not detected in our samples. In this study, total Chl *a* concentration measured by HPLC method (hereafter denoted as TChl *a*) was defined as the sum of Chl *a*, chlorophyllide *a*, and pheophorbide *a* (Table 1). Samples for the identification and enumeration of eukaryotic cells were collected at the surface and at the bottom of the euphotic zone, preserved in acidic Lugol's solution [*Parsons et al.*, 1984] and then stored in the dark at 4°C until analysis. Cells $> 2 \mu\text{m}$ were identified to the lowest possible taxonomic rank and enumerated under an inverted microscope (Wild Heerbrugg) equipped with phase contrast optics [*Lund et al.*, 1958].

2.2.3. Phytoplankton size structure

Samples were filtered onto 25 mm Whatman GF/F glass-fiber filters, $5 \mu\text{m}$ Nuclepore polycarbonate membranes and $20 \mu\text{m}$ Nitex screens for the determination of the Chl *a* biomass of pico- ($< 5 \mu\text{m}$), nano- ($5 - 20 \mu\text{m}$) and microphytoplankton ($> 20 \mu\text{m}$). After 24 h extraction in 90% acetone at 4°C in the dark, Chl *a* concentrations were determined on a 10-AU Turner Designs fluorometer (acidification method [*Parsons et al.*, 1984]). In addition, fluorometric measurements of Chl *a* retained on the GF/F filters (hereafter denoted as Chl *a*^{Fluo}) were used to provide a global view of the spatial distribution of phytoplankton biomass. The relative biomass of each size class determined

above was compared with HPLC pigment-derived classes methods [Vidussi *et al.*, 2001; Uitz *et al.*, 2006]. The relative biomass of small phytoplankton cells ($0.2 - 20 \mu\text{m}$) was underestimated by the pigment composition method since zeaxanthin (a tracer of picophytoplankton) and alloxanthin (a tracer of nanophytoplankton) were not detected in our samples. Hence, the phytoplankton size structure was determined from the fluorometric method.

2.2.4. Particulate and algal absorption measurements

At selected stations, samples (1.5 to 2.0 L) for the measurement of the spectral absorption of particulate matter were filtered under low vacuum onto 25 mm Whatman GF/F glass-fiber filters. Blank filters were made regularly by filtering distilled water onto GF/F filters. Filters were stored in Petri dishes and kept frozen in liquid nitrogen until laboratory analysis. The transmittance-reflectance (T-R) method was used to measure *in vivo* light absorption by aquatic particles retained on the filter [Tassan and Ferrari, 2002]. This method is recommended in coastal regions (Case 2 waters) containing highly scattering matter. The optical density (OD, dimensionless) of these filters, before ($\text{OD}_p(\lambda)$) and after ($\text{OD}_{na}(\lambda)$) methanol extraction [Kishino *et al.*, 1985], was measured using a dual beam Perkin-Elmer Lambda 2 spectrophotometer equipped with a 50 mm integrating sphere (Labsphere RSA-PE-20). Algal pigments from the filters were extracted using 95% methanol [Kishino *et al.*, 1985] since (1) no unextractable pigments were detected and (2) no significant difference between pigment extraction solvents (i.e. methanol, acetone [Bricaud and Stramski, 1990] and sodium hypochlorite [Tassan and Ferrari, 2002]) has been reported in the literature. Scans were conducted at 1 nm intervals from 300 to 800 nm at a speed of 240 nm min^{-1} . Baseline and null corrections were performed by subtracting the OD_f of a fully hydrated blank filter and the averaged OD_f values between 790 and 800 nm from $\text{OD}_p(\lambda)$ and $\text{OD}_{na}(\lambda)$ [Babin and Stramski, 2002]. The OD_p and OD_{na} coefficients were transformed into their equivalent OD value in suspension ($\text{OD}_{sus}(\lambda)$). The $\text{OD}_{sus}(\lambda)$ is a general and empirical relationship between the optical density of particles

retained on filters ($OD_s(\lambda)$) and particles in suspension ($OD_{sus}(\lambda)$) for mixed cultures and various filter types [Mitchell, 1990]. The particulate $a_p(\lambda)$ and non algal $a_{na}(\lambda)$ absorptions were obtained by equations given by Tassan and Ferrari [2002] using $OD_{sus}(\lambda)$, filtered volume of seawater and the area of the filter. The phytoplankton light absorption coefficient ($a_\phi(\lambda)$, m^{-1}) was determined using the following equation: $a_\phi(\lambda) = a_p(\lambda) - a_{na}(\lambda)$ (m^{-1}). The TChl α -specific absorption coefficient of phytoplankton ($a_\phi^*(\lambda)$, m^2 mg TChl α^{-1}) was calculated as: $a_\phi^*(\lambda) = a_\phi(\lambda)/TChl \alpha$, where TChl α is the total chlorophyll α concentration measured by HPLC (mg m^{-3} ; see Table 1). When TChl α values were not available, they were estimated from a linear regression between TChl α and Chl α^{Fluo} . For Chl α^{Fluo} concentrations ranging from 0.059 to 5.0 mg m^{-3} , the regression equation is: $TChl \alpha = 0.825(Chl \alpha^{Fluo})$ ($r^2 = 0.90$, $n = 62$) setting intercept equals to zero.

2.2.5. Colored dissolved organic matter (CDOM) absorption measurements

At selected stations, water samples were filtered using 0.2 μm Anotop® filters. The filtrates were kept in HCl-cleaned bottles at -20°C in the dark. The OD of CDOM ($OD_{cdom}(\lambda)$) was measured from 200 to 800 nm at 1 nm intervals using a Perkin-Elmer Lambda 2 spectrophotometer in a 10 cm quartz cell. Scan speed was 240 nm min^{-1} . The CDOM absorption coefficient ($a_{cdom}(\lambda)$) was calculated as: $a_{cdom}(\lambda) = 2.303(OD_{cdom}(\lambda) - OD_{cdom}(600))/0.1$ (m^{-1}), where $OD_{cdom}(600)$ is the averaged OD value between 590 and 600 nm [Fargion and Mueller, 2000].

2.2.6. Data processing and statistical analyses

The relative absorption contributions of phytoplankton (a_ϕ), non algal (a_{na}) and colored dissolved organic matter (a_{cdom}) to the total nonwater absorption (a_{t-w}) were calculated at five SeaWiFS wavelengths (Figure 2). The a_{t-w} is defined as: $a_{t-w}(\lambda) = a_\phi(\lambda) + a_{na}(\lambda) + a_{cdom}(\lambda)$ (m^{-1}). The Brunt-Väisälä frequency (N^2 in s^{-2}), a water stratification index, was computed according to Pond and Pickard [2005]: $N^2 = g \rho^{-1} (d\rho/dz)$, where g ($m s^{-2}$) is

the gravitational acceleration, ρ (kg m^{-3}) is the seawater density [Fofonoff and Millard, 1983] and z (m) is the depth. The mixed layer depth (Z_{MLD}) corresponds to the maximum value of N^2 . The depth interval for these calculations is 1 meter. Interquartile ranges, extents and medians of $a_\phi^*(\lambda)$ samples were calculated at eight SeaWiFS wavelengths (Figure 3). The outliers (i.e. values that are more than 1.5 times the interquartile range away from the interquartile range itself) that do not correspond to observed values of literature [Bricaud *et al.*, 1995, 1998; Babin *et al.*, 1996; Allali *et al.*, 1997; Matsuoka *et al.*, 2007; Roy *et al.*, 2008] were removed. The relationships between $a_\phi(\lambda)$ and TChl a were calculated according to the following equation: $a_\phi(\lambda) = A_\phi(\lambda) (\text{TChl } a)^{B_\phi(\lambda)} (\text{m}^{-1})$ [Bricaud *et al.*, 1998], where A_ϕ and B_ϕ are regression's constants. TChl a and $a_\phi(443)$ regressions were base 10 log-transformed. The *package effect* was estimated (hereafter denoted as $Q^*(675)$) using the ratio between Chl a -specific phytoplankton light absorption coefficients ($a_\phi^*(675)$) and specific absorption coefficient of Chl a in solution ($0.033 \text{ m}^2 \text{ mg Chl } a^{-1}$) at the wavelength 675 nm [Johnsen and Sakshaug, 2007; Roy *et al.*, 2008]. This ratio assumed that Chl a is the main light absorbing pigment at 675 nm. The ratio $Q^*(675)$ (dimensionless) ranging from 1 (unpackaged pigments) to 0.10 (strong packaging), where values above 1 indicate missing absorption terms [Bricaud *et al.*, 2004, Roy *et al.*, 2008]. The total concentration of pigments per cell also provided an estimation of *package effect* level.

Before performing parametric tests, the normality of distribution of the data was verified by the Lilliefors test. A one-way analysis of variance (ANOVA) and a multiple comparison of means using Tukey's HSD criterion were then conducted to find any significant differences ($p < 0.05$) between the four oceanographic provinces. Cluster analysis, the single method using the nearest neighbor by Euclidean distance, and multiple linear regressions ($y = a_1x_1 + a_2x_2 + b$) were used to determine the relationships between biological and/or physical variables. If the normality of a distribution was not confirmed, a nonparametric Kruskal-Wallis test was performed instead of the ANOVA. The p value is

only mentioned for comparison test. Statistical analyses were conducted using MATLAB software (version 7.1). Abbreviations are listed in Table 1. The following sections were determined by the data availability; vertical structures were only studied in the Canadian High Arctic and the seasonality variations only in the Amundsen Gulf.

Table 1. Symbols and abbreviations

Symbol	Definition	Unit
Chl α^{Fluo}	Chlorophyll α concentration measured by fluorometry	mg m ⁻³
[Chl α^{Fluo}] _{<i>i</i>}	Chlorophyll α concentration for parameter <i>i</i>	mg m ⁻³
$\langle \text{Chl } \alpha^{\text{Fluo}} \rangle_{\text{Zeu}}$	Integrated Chl α^{Fluo} over the euphotic zone	mg m ⁻²
TChl α	Total chlorophyll α concentration measured by HPLC (i.e. chlorophyll α (Chl α) + pheophorbide (Phide α) + chlorophyllide (Chlide α))	mg m ⁻³
Chl b	Chlorophyll b concentration (HPLC)	mg m ⁻³
TChl c	Total chlorophyll c concentration (HPLC) (i.e. chlorophyll c_1 (Chl c_1) + chlorophyll c_2 (Chl c_2) + chlorophyll c_3 (Chl c_3))	mg m ⁻³
PSC	Photosynthetic carotenoids (HPLC) (i.e. fucoxanthin (Fuco) + peridinin (Peri) + 19'-butanoyloxyfucoxanthin (BFU) + 19'-hexanoyloxyfucoxanthin (HFU) + $\beta\epsilon$ -carotene)	mg m ⁻³
PPC	Photoprotective carotenoids (HPLC) (i.e. diadinoxanthin (DD) + diatoxanthin (DT) + alloxanthin (Allo) + zeaxanthin (Zea) + $\beta\beta$ -carotene)	mg m ⁻³
AccP	Total accessory pigments (HPLC) (i.e. Chl b + TChl c + PSC + PPC)	mg m ⁻³
SCM	Subsurface chlorophyll maximum	mg m ⁻³
λ	Wavelength	nm
k	Vertical light attenuation coefficient	m ⁻¹
$a_p(\lambda)$	Absorption coefficient of particles	m ⁻¹
$a_\phi(\lambda)$	Absorption coefficient of phytoplankton	m ⁻¹
$a_{\text{na}}(\lambda)$	Absorption coefficient of non algal material	m ⁻¹
$a_{\text{cdom}}(\lambda)$	Absorption coefficient of colored dissolved organic matter	m ⁻¹
$a_{\text{t-w}}(\lambda)$	Total nonwater absorption ($a_\phi(\lambda) + a_{\text{na}}(\lambda) + a_{\text{cdom}}(\lambda)$)	m ⁻¹
$a_\phi^*(\lambda)$	Chl α -specific coefficient absorption of phytoplankton ($a_\phi(\lambda)/ \text{TChl } \alpha$)	$\text{m}^2 \text{ mg TChl } \alpha^{-1}$
$Q^*(675)$	Package effect factor ($a_\phi^*(675)/ 0.033 \text{ m}^2 \text{ mg Chl } \alpha^{-1}$)	-
$B_\phi, A_\phi(443)$	Constants in the regression between $a_\phi(443)$ and TChl α	-
N^2	Brunt-Väisälä frequency	s ⁻²
Z_{MLD}	Mixed layer depth	m
$Z \leq Z_{50\%}$	Depth over or equal to 50% of surface irradiance (surface samples)	m
$Z > Z_{50\%}$	Depth between 1 and 50% of surface irradiance	m

2.3 RESULTS AND DISCUSSION

2.3.1. Absorption Budget

The light absorption budget can be used to characterize the water color. This budget is composed of the relative absorption of $a_\phi(\lambda)$, $a_{na}(\lambda)$ and $a_{cdom}(\lambda)$ (i.e. divided by the total nonwater absorption $a_{t-w}(\lambda)$). Table 2 shows that near the phytoplankton absorption maximum, at 443 nm, the CDOM is generally the major light absorbing compound in surface waters of all regions, with $a_\phi(443)$ only contributing to 11% of total nonwater absorption in the Amundsen Gulf, 21% in the Canadian Arctic Archipelago and 28% in northern Baffin Bay. During the fall, the absorption by non algal ($a_{na}(443)$) matter was relatively weak except in the Amundsen Gulf (21%). In return, the contribution of phytoplankton to light absorption was higher (21%) than non algal matter (7%) during spring/summer in this region. In the Canadian High Arctic, the important contribution of CDOM (the Amundsen Gulf = 70%, Canadian Arctic Archipelago = 72% and northern Baffin Bay = 60%) reflects the global influence of freshwater pathways from Arctic rivers through the area [Macdonald *et al.*, 2005].

In the northern Baffin Bay, surface currents bring saltier Atlantic waters along the Greenland coast while there is a sustained southerly flow of fresher water along Ellesmere Island on the western side [Melling *et al.*, 2001] characterized by higher CDOM concentrations. Near the Amundsen Gulf, the principal source of CDOM is the Mackenzie River outflow located 200 km to the west ($418 \text{ km}^3 \text{ y}^{-1}$) [Carmack *et al.*, 2004; Macdonald *et al.*, 2005; Lammers *et al.*, 2001]. The highest CDOM proportion in percentage was observed in the Hudson Bay system (80%), a large estuarine-like inland sea that receives 760 km^3 of freshwater per year from its tributaries [Déry *et al.*, 2011]. The $a_\phi(443)$ coefficients only contributing to 13% of absorption budget in the Hudson Bay (except for station AN01) and up to 65% in the Hudson Strait (Table 2).

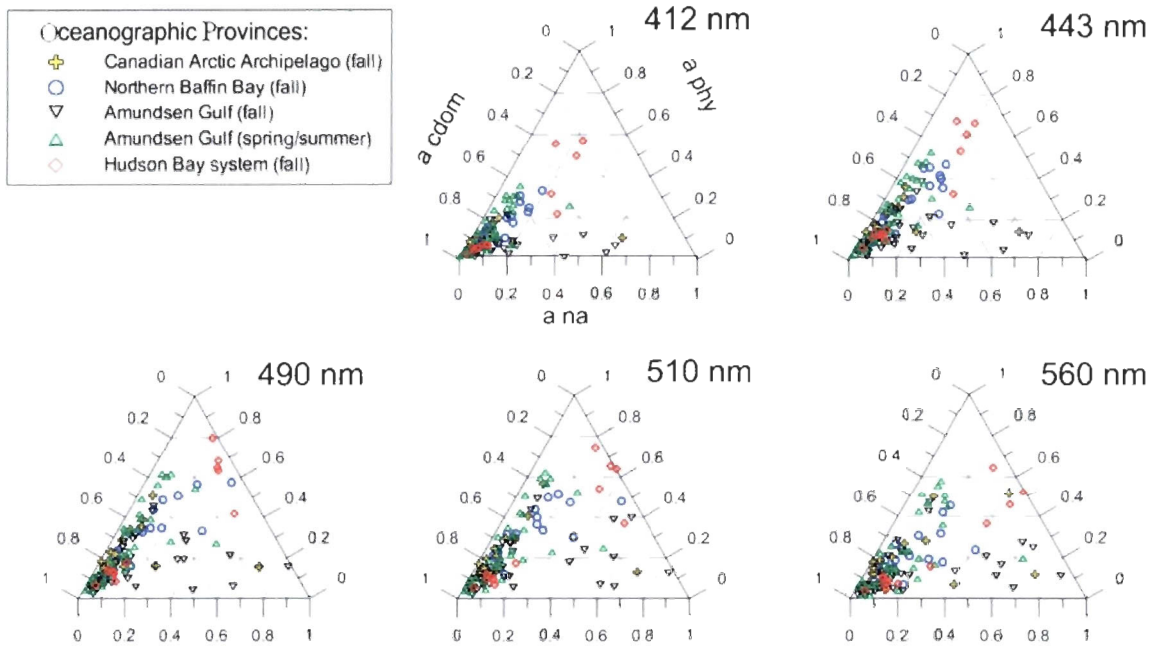


Figure 2. Relative contributions of phytoplankton (a_ϕ), non algal matter (a_{na}) and colored dissolved organic matter (a_{cdom}) to total non-water absorption at five SeaWiFS wavelengths in the four oceanographic provinces (all depths). Full grey lines = a_{cdom} , horizontal dashed lines = a_ϕ and diagonal dashed lines = a_{na} .

This spatial variability reflects the pattern of freshwater inflows located mostly in the southern and eastern portions of the Bay while the Hudson Strait region is more influenced by inputs coming from Atlantic and Arctic [Granskog *et al.*, 2011]. Even though the surface waters CDOM absorption ($0.013 - 0.29 \text{ m}^{-1}$) are in the range of European coastal waters ($0.004 - 0.7 \text{ m}^{-1}$) [Babin *et al.*, 2003], the contributions in percentage are higher. Those high proportions of CDOM are also observed at other wavelengths (412, 443, 490, 510 and 560 nm), used in the development of ocean color remote sensing algorithms, and also at all depths (Figure 2).

Table 2. Phytoplankton (a_ϕ), non algal material (a_{na}) and colored dissolved organic matter (a_{cdom}) absorption coefficients at 443 nm, their relative contributions to the total nonwater absorption (a_{t-w}) and chlorophyll *a* concentration measured by fluorometry (Chl a^{Fluo}) in surface waters ($Z \leq Z_{50\%}$) of the four oceanographic provinces. Average, SD (in parentheses) and range are shown; n = number of observations.

Province	Year Season	$a_\phi(443)$ (m ⁻¹)	$a_\phi(443)/a_{t-w}(443)$ (%)	$a_{na}(443)$ (m ⁻¹)	$a_{na}(443)/a_{t-w}(443)$ (%)	$a_{cdom}(443)$ (m ⁻¹)	$a_{cdom}(443)/a_{t-w}(443)$ (%)	n	Chl a^{Fluo} Range (mg m ⁻³)
Amundsen Gulf (this study)	2007 Fall	0.011 (0.005)	11	0.021 (0.021)	21	0.068 (0.040)	68	10	0.1-0.7
Amundsen Gulf (this study)	2008 Spring & summer	0.019 (0.015)	21	0.006 (0.003)	7	0.063 (0.031)	72	20	0.06-0.5
Canadian Arctic Archipelago (this study)	2007 Fall	0.019 (0.008)	21	0.013 (0.04)	14	0.058 (0.015)	65	6	0.3-0.4
Northern Baffin Bay (this study)	2007 Fall	0.031 (0.028)	28	0.013 (0.010)	12	0.067 (0.017)	60	10	0.1-3.0
Hudson Strait - Hudson Bay* (this study)	2005 Fall	0.055 (0.013) 0.045 (0.020)	65 13	0.014 ((0.015) 0.026 (0.003)	17-7	0.015 (0.005) 0.29 (0.21)	18 80	2 13	0.3-0.8 0.2-1.0
Chukchi Sea, Western Arctic Ocean [Mastuoka et al., 2011] (all depths)	2002 Spring: Summer: Fall:	0.017 0.022 0.016	22 29 18	0.011 0.012 0.006	14 16 9	0.049 0.041 0.066	64 55 73	90 110 179	0.05-10
Coastal waters around Europe [Babin et al., 2003] (surface waters)	1997-1998 Spring, summer & fall	0.005-1.0	36	0.001-1.0	22	0.007-0.7	41	330	0.002-30

* Including stations 15 and 16

2.3.2. Regional variability

Spatial variability was assessed using only the data taken at the surface during the fall period in order to include the Hudson Bay. Figure 3 shows the mean specific phytoplankton absorption coefficient spectra for each province with descriptive statistics at eight SeaWiFS wavelengths. The two absorption maxima of Chl *a* around 440 and 675 nm are easy to identify in the $a_{\phi}^*(\lambda)$ spectra. Absorption maxima of Chl *b* at 465 nm and TChl *c* at 461 nm [Hoepffner and Sathyendranath, 1991; Bricaud *et al.*, 2004] combined with photoprotective carotenoids (PPC) absorption maximum at 460 nm and the photosynthetic carotenoids (PSC) absorption maximum at 490 nm [Bricaud *et al.*, 2004] also contribute to the observed spectral shapes. The $a_{\phi}^*(443)$ average was lower ($p < 0.05$) in the Canadian High Arctic than in the Hudson Bay system. In the Hudson Bay system the observed values are similar to the $a_{\phi}^*(443)$ coefficients measured in 1) the Black Sea [Dmitriev *et al.*, 2009], 2) the North Atlantic waters dominated by pico- and nanophytoplankton [Bricaud *et al.*, 2004] and 3) the Labrador Sea [Cota *et al.*, 2003].

The spectra measured are relatively flattened in the Canadian High Arctic. Thus, the blue-to-red ratio averages $a_{\phi}(443):a_{\phi}(675)$ are also generally low (Figure 4a) [Bricaud *et al.*, 1995; Babin *et al.*, 2003], especially in the Amundsen Gulf (1.8, SD = 0.3) and northern Baffin Bay (1.5, SD = 0.3) (Figure 4b). Those ratios are similar to those observed in the Atlantic sector of the Southern Ocean (1.6 – 2.2) [Bracher and Tilzer, 2001]. The highest averaged $a_{\phi}(443):a_{\phi}(675)$ ratios have been observed in the Canadian Arctic Archipelago (2.0, SD = 0.3) and Hudson Bay system (2.5, SD = 0.7) (Figure 5b), but that last province had a really high spatial variability (Figure 4b). Consequently, the $a_{\phi}(443)$ and $a_{\phi}(675)$ coefficients are well correlated together in the Canadian High Arctic ($r^2 = 0.93$) but not in the Hudson Bay system ($r^2 = 0.17$).

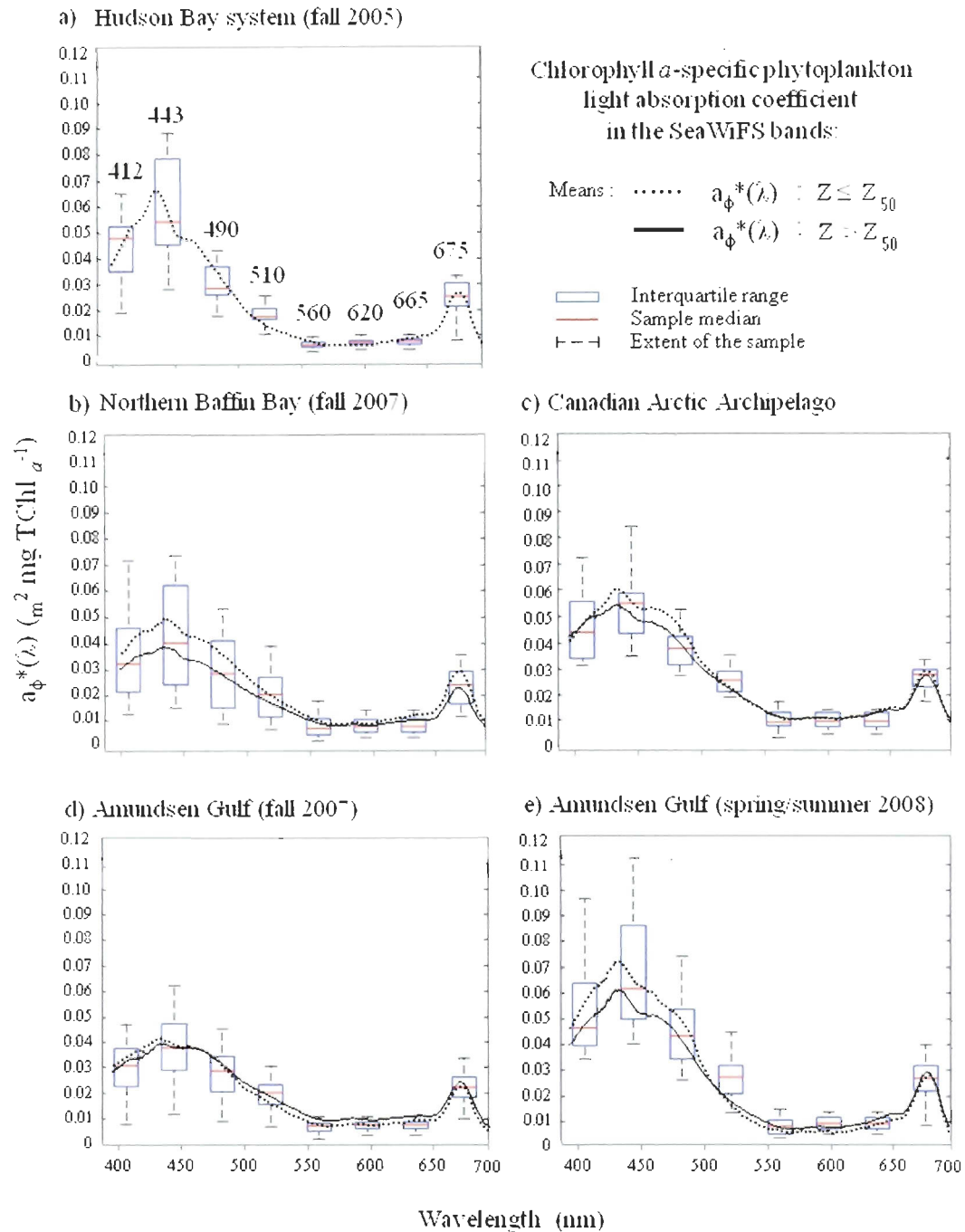


Figure 3. Box plots of the total Chl α -specific light absorption by phytoplankton ($a_{\phi}^*(\lambda)$) of each oceanographic province at eight SeaWiFS wavelengths. Descriptive statistics were calculated for all depths, except in the Hudson Bay system where only surface waters had been sampled. Spectra averages, between 400 and 700 nm, are shown at the surface for $Z \leq Z_{50}$ (i.e. $\geq 50\%$ of surface irradiance) and deeper waters for $Z > Z_{50}$ (i.e. from 50% to 1% of surface irradiance).

The spectral flattening could be caused by the *package effect*, closely associated with the light availability and the cell size [Bricaud and Stramski, 1990; Babin et al., 2003]. The averaged $Q^*(675)$ values, decreasing as the *package effect* level increases, were lower in the Amundsen Gulf (0.70) and northern Baffin Bay (0.73) than in the Canadian Arctic Archipelago (0.82) and Hudson Bay system (0.77). More precisely, the total concentration of pigments (i.e. the sum of all different pigment concentrations) per cell was higher ($p << 0.05$) in the Canadian High Arctic ($0.32 - 3.8 \text{ pg cell}^{-1}$) than in the Hudson Bay system ($0.21 - 1.44 \text{ pg cell}^{-1}$). This indicates that the cells are potentially shade-adapted in the Canadian High Arctic during fall producing more pigments per cell, creating the *package effect* and reducing the $a_\phi^*(443)$ coefficients. The proportions of accessory pigments are also a little high in this region (Figure 6a). This could explain why the values of $a_\phi^*(443)$ are directly proportional ($r^2 = 0.73$) to $Q^*(675)$ in the Canadian High Arctic but are not ($r^2 = 0.11$) in the Hudson Bay system.

For the Hudson Bay system, the best linear regression fit for $a_\phi^*(443)$ used not only the index of the *package effect* $Q^*(675)$ but also the concentrations of accessory pigments ($\text{AccP}^* = \text{AccP}/\text{TChl } a$) as independent variables ($r^2 = 0.74$). The small cell size experiencing a weak *package effect* level, the high proportions of small cells ($< 5 \mu\text{m}$) in the Canadian Arctic Archipelago (82%) and in the Hudson Bay system (67%), compared to the Amundsen Gulf (60%) and northern Baffin Bay (49%), could also explain the relatively high $Q^*(675)$ values observed in those regions (Figure 5c). The presence of larger cells and higher *package effect* in the Baffin Bay and the western Arctic Ocean is probably related to higher nutrient levels availability [Hill and Cota, 2005; Tremblay et al., 2006; Klein et al., 2002; Lovejoy et al., 2002].

Assuming that the *package effect* is not totally overwhelming the pigment effect, the pigment composition could also explain some differences between phytoplankton specific absorption coefficients. The $\text{TChl } a$ -specific concentrations of PSC^* ($\text{PSC}^* = \text{PSC}/\text{TChl } a$) in the Amundsen Gulf (0.70), Canadian Arctic Archipelago (0.45) and northern Baffin Bay (0.73) (Figure 6d) correspond to the highest values measured in the North Atlantic waters during the February to May time period with a population dominated by both nano- and

picophytoplankton [Bricaud *et al.*, 2004]. Those PSC* proportions are also higher than what was measured in the Hudson Bay system (0.37). Inversely, the TChl *a*-specific concentrations of PPC* ($PPC^* = PPC/TChl\ a$) were clearly smaller ($p << 0.05$) in the Amundsen Gulf (0.09), northern Baffin Bay (0.10) and Canadian Arctic Archipelago (0.10) than in the Hudson Bay system (0.22) (Figure 5d). The PPC* values in the Hudson Bay system were in the range of observations made in coastal waters of temperate regions (Figure 6b) [Babin *et al.*, 2003], while those of the Canadian High Arctic were similar to values measured in arctic marine phytoplankton adapted to low incident light [Matsuoka *et al.*, 2011]. Those results highlight the fact that the high $a_\phi^*(443)$ observed in the Hudson Bay system are related to higher proportions of PPC (absorbing at shorter wavelengths than PSC).

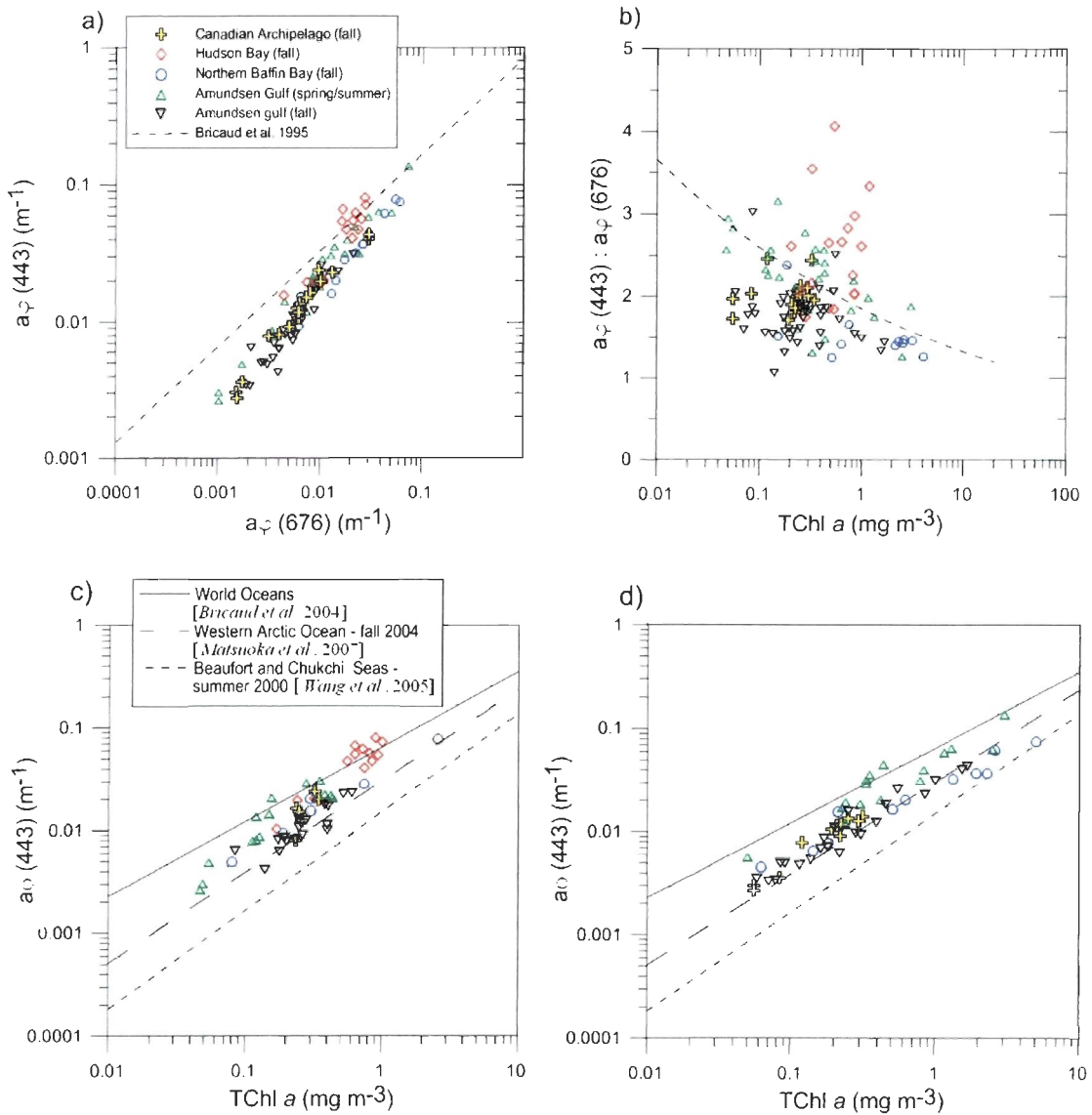


Figure 4. Variations of (a) the absorption coefficient of phytoplankton $a_\phi(443)$ as a function of the absorption coefficient of phytoplankton $a_\phi(676)$ and (b) the ratio of $a_\phi(443)$ to $a_\phi(676)$ as a function of the total Chl a concentrations for all depths, shown in log scale. Dashed lines of figures (a) and (b) represent the regression lines of Babin et al. [2003]. The (c) $a_\phi(443)$ coefficient as a function of the total Chl a concentrations at the surface (i.e. $\geq 50\%$ of surface irradiance) and (d) deeper waters (i.e. from 50% to 1% of surface irradiance) are shown. In (c) and (d), regression lines of Wang et al. [2005] for the Beaufort and Chukchi seas, Matsuoka et al. [2007] for the western Arctic Ocean and Bricaud et al. [2004] for the World Oceans are drawn for comparison. Note that the absorption coefficient was measured at 440 nm for surface waters in Bricaud et al. [2004], and for all depths in Matsuoka et al. [2007] and Wang et al. [2005].

Moreover, the main pigment contributions to PPC in the Canadian High Arctic were, on average, the diadinoxanthin ($DD/TChl\alpha = DD^* = 0.05$, $SD = 0.02$) with no or very low concentrations of alloxanthin (Allo) and zeaxanthin (Zea). In the Hudson Bay system, the averages of DD^* (0.08 , $SD = 0.02$), $Allo^*$ ($Allo/TChl\alpha = 0.06$, $SD = 0.03$) and Zea^* ($Zea/TChl\alpha = 0.05$, $SD = 0.05$) were relatively higher. This suggests once again that the Canadian High Arctic's phytoplankton community could be acclimated to low light conditions (i.e. epoxidization of DT into DD under low light irradiance) [Demers *et al.*, 1991; Kashino and Kudoh, 2003; Lavaud *et al.*, 2004; Goss and Jackob, 2010]. The xanthophylls cycle (i.e. response to sudden change in irradiance) could be more active in the Hudson Bay system, containing more xanthophylls pigments [Kashino *et al.*, 2002] and a more adequate nutrients supply [Dubinsky and Stambler, 2009; Moreno *et al.*, 2012].

A cluster analysis of TChl α -specific light absorption by phytoplankton, cell size and $Q^*(675)$ values divides the Canadian High Arctic dataset in two major groups characterized by: 1) a relatively high proportion of picophytoplankton, low *package effect* and high $a_\phi^*(443)$ and 2) a relatively low proportion of picophytoplankton, high *package effect* and low $a_\phi^*(443)$ (Figure 5a, 5c). Using the most abundant and quantifiable pigments determined by HPLC, we also divided the phytoplankton community into two groups. The first group includes prasinophyceae and chlorophycea (Chl *b* + Prasino) and the second group includes bacillariophyta, dinophyta, prymnesiophycea and chrysophycea (TChl *c* + Fuco + Diadino) [Jeffrey *et al.*, 1997; Vidussi *et al.*, 2004]. These two groups basically represent green (i.e. containing Chl *b*) and red algae (i.e. containing Chl *c*) and are correlated with the salinity (Figure 5f).

The second cluster analysis showed that the group 1 is dominated by algae containing a high proportion of Chl *b** ($Chl\alpha/b/TChl\alpha$) + Prasino* ($Prasino/TChl\alpha$) while group 2 is dominated by algae containing high proportion of Fuco* ($Fuco/TChl\alpha$) + TChl *c** ($TChl\alpha/c/TChl\alpha$) (Figure 7). The first group includes stations in northeastern Amundsen Gulf (stns. 405, 1100, 1200, 1902 and 1908), Canadian Arctic Archipelago (stns. 301, 302, 308, 309 and 310) and northwestern Baffin Bay (stns. 101 and 134). The second group includes stations in the middle and southwest of the Amundsen Gulf (stns. 407, 408, 1110, 1116 and

1216) as well as those in the northeastern Baffin Bay (stns. 108, 111 and 115). The observed spatial differences of optical properties in the Amundsen Gulf could be related to the general anticyclonic circulation pattern in the area with water entering the gulf along Banks Island and exiting at the Cape Bathurst [Lanos, 2009]. The significantly highest Fuco* average (0.50, SD = 0.1) was correlated with the presence of diatoms (microscopy counts) in northern Baffin Bay ($r^2 = 0.76$). These results agree with previous works which showed that diatoms dominated the community along the Greenland coast while waters along the Canadian coast mostly contained flagellates [Vidussi *et al.*, 2004]. In summary, our results show that there exists spatial variability of the phytoplankton optical properties between the different oceanographic provinces and that the provinces cannot be considered as spatially homogeneous.

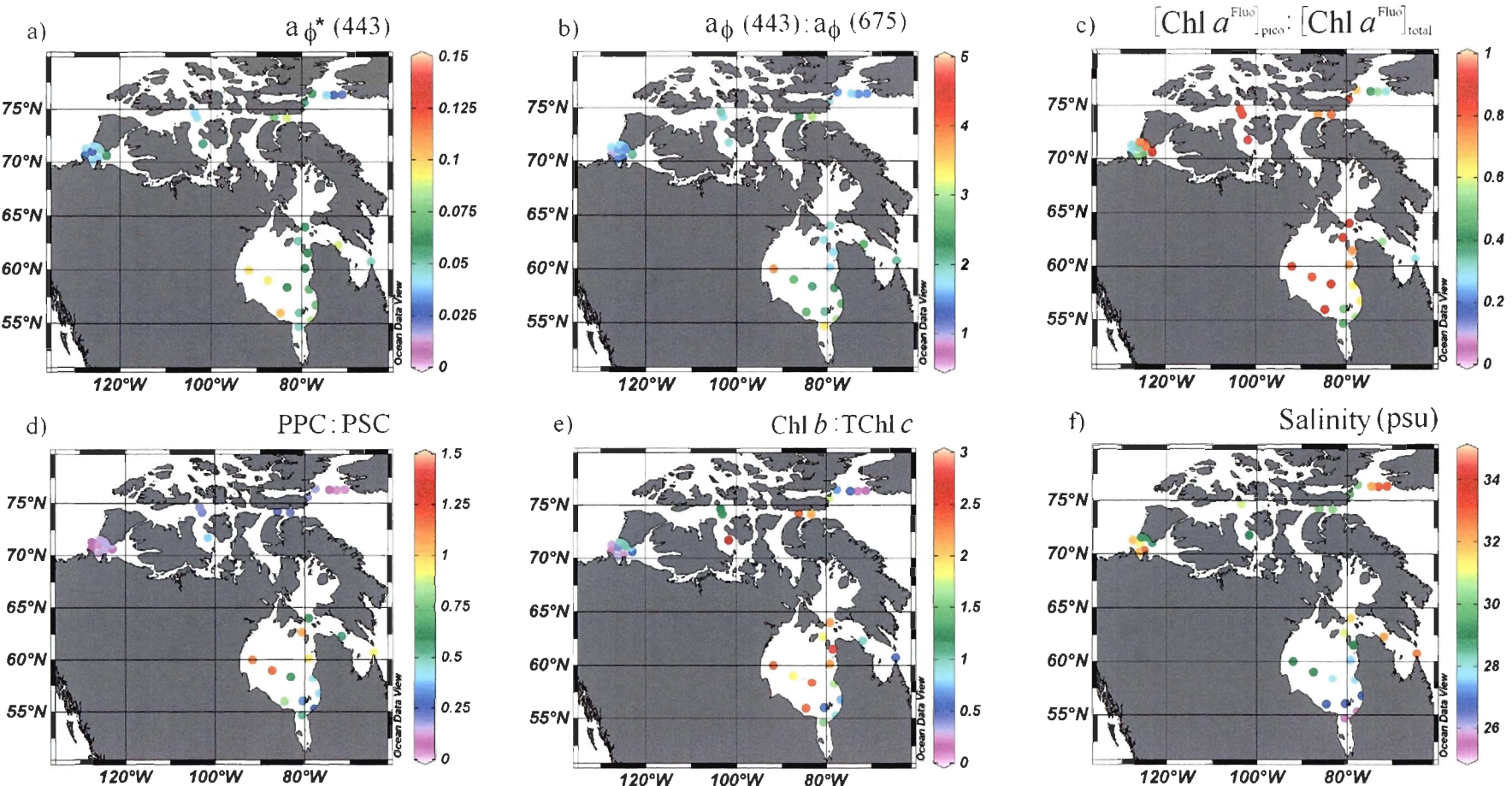


Figure 5. Spatial variations of the (a) total Chl α -specific phytoplankton light absorption coefficient $a_{\phi}^*(443)$, (b) blue-to-red ratio $a_{\phi}(443):a_{\phi}(675)$, (c) relative proportion of picophytoplankton, (d) ratio of photoprotective carotenoids (PPC) and photosynthetic carotenoids (PSC), (e) ratio of Chl b and TChl c and (f) salinity in surface waters (i.e. $\geq 50\%$ of surface irradiance) of the Canadian Arctic during fall.

2.3.3. Vertical variability

Due to data availability, the vertical structures during fall were studied in the Canadian High Arctic only. Previous works conducted in Arctic seas have shown that the subsurface chlorophyll maximum (SCM) depth varies generally with the vertical water column stratification and nutrient supply rather than with the light availability [Tremblay *et al.*, 2002, 2008; Martin *et al.*, 2010]. Our results confirms this as there was also no clear relationship between the SCM depths and light attenuation coefficients (k) ($r^2 = 0.12$). Over the three Canadian High Arctic provinces, the averaged pycnocline depth (24 m, SD = 16) was shallower (44 m, SD = 15) than the averaged euphotic depth ($Z_{eu} = 1\%$ of surface irradiance). There were, however, some regional variations of the averaged euphotic depth. The SCMs were located below (40%) or above (60%) the pycnocline and were ranging from 5 to 62 m with a mean value of 25 m (SD = 16). This high variability in the vertical location of the SCM is mostly explained by the relatively deep SCMs observed in the Amundsen Gulf and northern Baffin Bay, which develop during the summer near the bottom of the mixed layer as nutrients become depleted [Carmack *et al.*, 2004, Martin *et al.*, 2010], and the presence of a near surface SCMs in the Canadian Arctic Archipelago (i.e. located above the pycnocline and above 10 meters).

In the temperate oceans, Uitz *et al.* [2006] proposed phytoplankton biomass vertical distribution models for stratified-oceanic waters, with euphotic zone depth (Z_{eu}) thicker than the mixed layer depth (Z_{MLD}) ($Z_{eu}/Z_{MLD} > 1$), and for mixed waters. Our results indicated that the stratified waters model doesn't work in the Canadian High Arctic (not shown). However, the mixed waters model provides a better estimation of integrated Chl a , when the high phytoplankton biomasses ($\langle \text{Chl } a^{\text{Fluo}} \rangle_{Zeu}$) measured in the northern Baffin Bay were included. The best regression obtained for the three provinces of the Canadian High Arctic was: $\langle \text{Chl } a^{\text{Fluo}} \rangle_{Zeu} = 37.75[\text{Chl } a^{\text{Fluo}}]_{\text{surf}}^{(0.893)}$ ($r^2 = 0.74$), which is similar to the Uitz *et al.* [2006]'s mixed waters model.

The presence of the pycnocline into the euphotic zone with a closely associated SCM below or above it could lead to different phytoplankton communities with different photoacclimation properties along the water column [Babin *et al.*, 2003; Dubinsky and Stambler, 2009]. During the fall, the $a_\phi^*(443)$ averaged values were higher in surface waters (above 50% of surface irradiance) than deeper waters (Figure 3), except in the Amundsen Gulf. The regressions between $a_\phi(443)$ and TChl a (Table 3, Figure 4c and 4d) also show that specific light absorption tends to decrease with depth. Those regressions between both variables were generally similar to those observed in the western and southeastern Beaufort Sea during fall [Matsuoka *et al.*, 2007, 2009] and temperate ocean [Bricaud *et al.*, 2004] (Figure 4c).

The *package effect* index $Q^*(675)$ was slightly higher, not significantly ($p > 0.05$), in surface waters than deeper waters respectively in the Amundsen Gulf (0.70 and 0.66, $p = 0.93$), Canadian Arctic Archipelago (0.82 and 0.80, $p = 0.19$) and northern Baffin Bay (0.73 and 0.63, $p = 0.17$). For those provinces, the $Q^*(675)$ and $a_\phi^*(443)$ are well correlated together at the SCM ($r^2 = 0.90$) while the correlation was weaker for surface waters ($r^2 = 0.73$). The smallest $Q^*(675)$ values were observed for the highest TChl a values measured at the SCMs in the northern Baffin Bay (Figure 6c). The total concentration of pigments per cell was higher (not significantly, $p = 0.18$) in surface waters ($0.32 - 3.8 \text{ pg cell}^{-1}$) than in deeper waters ($0.82 - 5.4 \text{ pg cell}^{-1}$) of the Canadian High Arctic. This also indicates an increase of the *package effect* level with depth. Consequently, the spectra are relatively more flattened in deep waters, diminishing the blue-to-red ratios $a_\phi(443):a_\phi(675)$.

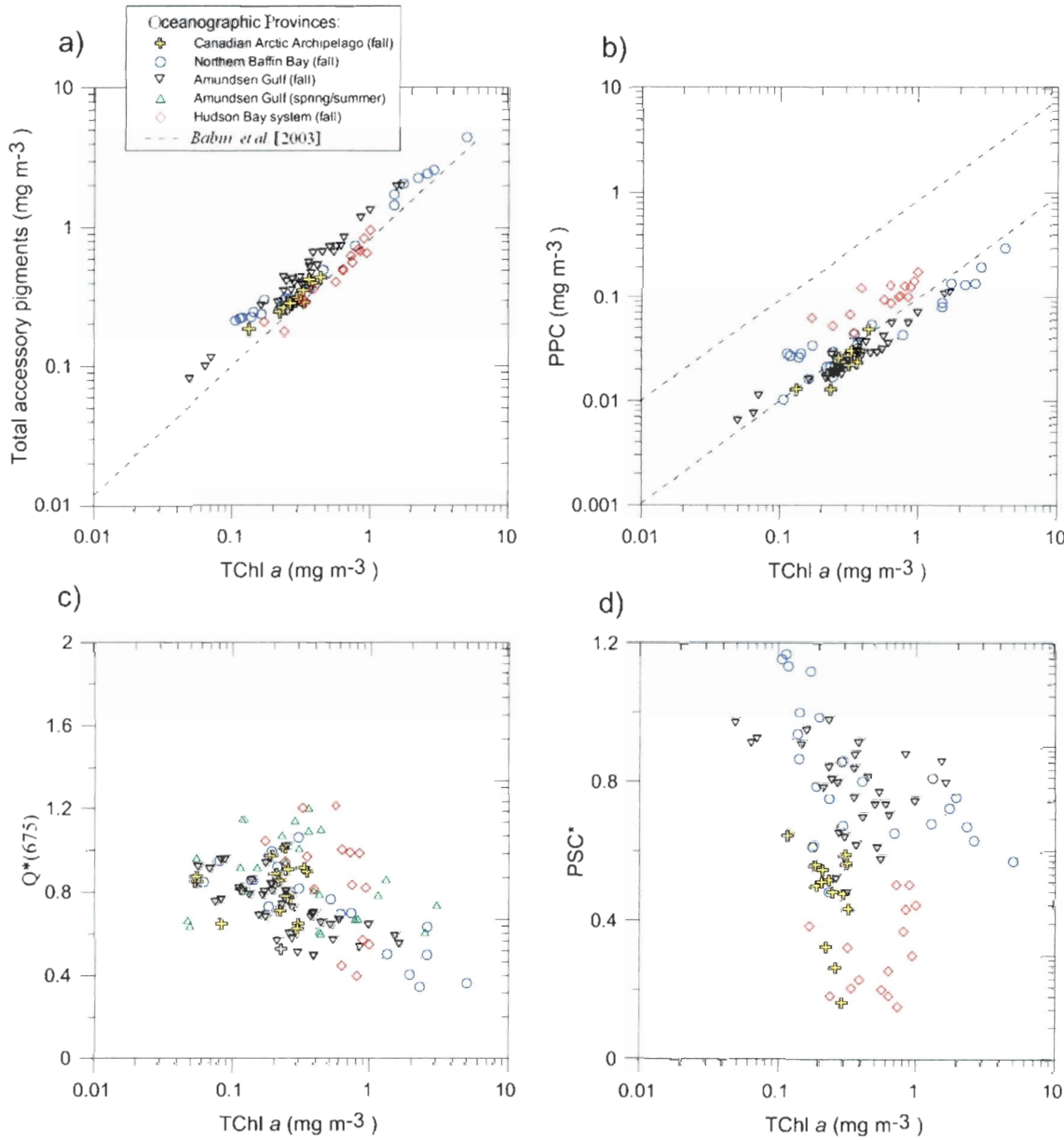


Figure 6. Relationships between total Chl *a* concentration and (a) total accessory pigments (AccP), the regression of our study corresponds to: $\text{AccP} = 0.813(\text{TChl } a)^{0.954}$ ($r^2 = 0.92$), (b) photoprotective carotenoids (PPC), (c) *Package effect* index $Q^*(675)$ and (d) total Chl *a*-specific photosynthetic carotenoids (PSC* = PSC/TChl *a*) in the four oceanographic provinces. Dashed lines represent in (a) regression and (b) approximated range measured by Babin et al. [2003]. Grey boxes represent the Bricaud et al. [2004]'s observation in North Atlantic waters dominated by small cells (February to May).

Overall, the spatial variation (see section 3.2) of averaged $a_\phi^*(443)$ appears to be stronger than the vertical variation, caused here by the cell size distribution. The dominance of small cells is particularly strong in the Canadian Arctic Archipelago's euphotic zone in the surface layer and deep layers (respectively 82% and 84%). The proportion of small cells ($[Chl\ \alpha^{Fluo}]_{pico}$) is weaker in the surface layer and deep layers of the Amundsen Gulf (respectively 60% and 49%) and northern Baffin Bay (respectively 49% and 45 %). The multiple comparison test of PSC*, Chl b^* and TChl c^* averages at the SCMs has also showed that pigment compositions were similar to surface waters but different per region (Figure 7); respectively the Amundsen Gulf system (0.98, 0.22 and 0.44), northern Baffin Bay (0.91, 0.12 and 0.33) and Canadian Arctic Archipelago (0.47, 0.42 and 0.25) (see section 3.2). The proportion of Fuco* was increasing throughout the middle of Baffin bay (Figure 7c) where the highest proportion of diatoms in the Canadian High Arctic's SCMs was observed (64%).

The grouping of stations by the cluster analysis at the SCM was similar to the grouping obtained for surface waters, except in the northern Baffin Bay where Q*(675), $a_\phi^*(443)$ and proportion of $[Chl\ \alpha^{Fluo}]_{pico}$ decreases throughout the middle of the bay (stns. 108 and 111). Light microscopy showed that those SCMs were dominated by diatoms, as opposed to the Amundsen Gulf where flagellates were dominant. In the Amundsen Gulf, the increase of TChl $c/Chl\ b$ and Fuco* ratio toward the southwest is particularly evident at the SCM (Figure 7a). In this area, the vertical stratification index (N^2) was low ($0.67 - 2.3 \times 10^{-3}\ s^{-2}$) compared to northeast part of Amundsen Gulf (N^2 of $1.5 - 5.5 \times 10^{-3}\ s^{-2}$). The stratification was also stronger in the Canadian Arctic Archipelago (N^2 of $1.3 - 5.6 \times 10^{-3}\ s^{-2}$) than in the northern Baffin Bay (N^2 of $0.52 - 1.8 \times 10^{-3}\ s^{-2}$) where the greatest biomass was observed. Those results show that the physical water column structure is the main factor affecting the phytoplankton biomass along the water column but with important spatial variations (see section 3.2).

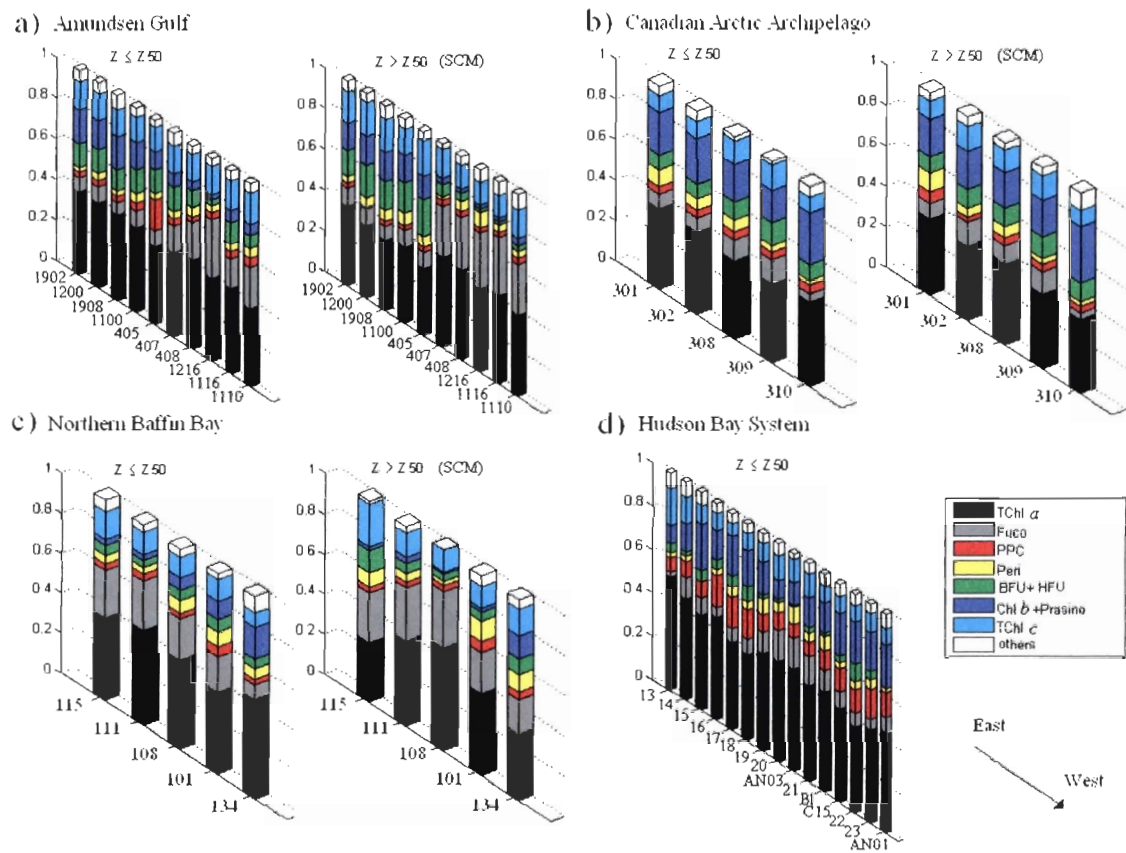


Figure 7. Relative contribution of the main marker pigments to total pigment concentration (weight-to-weight) in the (a) northern Baffin Bay, (b) Canadian Arctic Archipelago, (c) Amundsen Gulf and (d) Hudson Bay system for surface ($Z \leq Z_{50\%}$) and deeper waters ($Z > Z_{50\%}$) of the euphotic zone during fall. See Table 1 for pigment abbreviations.

Table 3. Constants for the power law regression $a_\phi(443) = A_\phi(443)[\text{TChl } a]^{B_\phi(443)}$ at 443 nm for surface ($Z \leq Z_{50\%}$) and deeper waters ($Z > Z_{50\%}$). Regressions including all depths are shown where r^2 is the coefficient of determination, n is the number of observations. Range, mean and SD of TChl a used for the regression are presented for each province. No regression has been calculated for the Canadian Arctic Archipelago; the range of TChl a in surface waters was too short.

	Period and Depth	$A_\phi(443)$	$B_\phi(443)$	r^2	n	TChl a Range (mg m^{-3})	Mean (SD)
Amundsen Gulf	Fall 2007						
	$z \leq z_{50\%}$:	0.0307	0.800	0.75	17	0.09-0.61	0.29 (0.14)
	$z > z_{50\%}$:	0.0301	0.786	0.94	22	0.06-1.7	0.39 (0.46)
Amundsen Gulf	All depths:	0.0302	0.788	0.90	39	0.06-1.7	0.35 (0.36)
	Spring-summer 2008						
	$z \leq z_{50\%}$:	0.0692	0.951	0.85	14	0.05-0.43	0.20 (0.14)
Canadian Arctic Archipelago	$z > z_{50\%}$:	0.0508	0.706	0.86	16	0.05-3.0	0.79 (0.85)
	All depths:	0.0534	0.803	0.88	30	0.05-3.0	0.51 (0.67)
	Fall 2007						
Northern Baffin Bay	$z \leq z_{50\%}$:	-	-	-	6	0.23-0.34	0.27 (0.05)
	$z > z_{50\%}$:	0.0462	0.950	0.95	11	0.06-0.31	0.18 (0.09)
	All depths:	0.0543	1.020	0.90	17	0.06-0.34	0.21 (0.09)
Hudson Bay system	Fall 2005						
	$z \leq z_{50\%}$:	0.0751	1.11	0.89	15	0.17-1.0	0.61 (0.27)
	Total Canadian High Arctic	Fall 2007					
	$z \leq z_{50\%}$:	0.0360	0.828	0.80	29	0.08-2.6	0.40 (0.47)
	$z > z_{50\%}$:	0.0282	0.717	0.94	44	0.06-5.0	0.59 (0.94)
	All depths:	0.0301	0.736	0.90	73	0.06-5.0	0.50 (0.78)
Total Canadian Arctic	All seasons						
	All depths:	0.0403	0.819	0.83	118	0.05-5.0	0.52 (0.71)
World Oceans [Bricaud et al., 2004]	Spring/summer/ fall 1986-1996						
	$z < z_{50\%}$:	0.0654	0.728	0.93	596	0.02 - 12	-
	All depths:	0.0378	0.627	0.90	1166	0.02 - 12	
Western Arctic Ocean [Matsuoka et al., 2011]	Spring:	0.0323	0.466	0.63	89	0.03 - 10	
	Summer:	0.0293	0.557	0.78	114	0.04 - 9.0	-
	Fall: (All depths)	0.0293	0.809	0.80	179	0.04 - 8.0	

2.3.4. Seasonality

Seasonal variability can only be assessed using data from the Amundsen Gulf and close by stations. It has already been noted that the specific light absorption usually decreases when the spring phytoplankton bloom occurs in temperate waters [Devred *et al.*, 2006; Roy *et al.*, 2008] as a result of the larger cell size and *package effect* increases. This decrease of $a_{\phi}^*(443)$ coefficients has also been observed in the euphotic zone of the Amundsen Gulf, from the beginning to the end of the open water season. The highest averaged $a_{\phi}^*(443)$ values observed during the spring/summer period ($0.068 \text{ m}^2 \text{ mg TChl } a^{-1}$, SD = 0.028) significantly decreased ($p << 0.05$) at all depths during the fall period ($0.042 \text{ m}^2 \text{ mg TChl } a^{-1}$, SD = 0.011). Moreover, the blue-to-red ratio during spring/summer was highly variable (Figure 4b).

This indicates that $a_{\phi}(443)$ is probably not only influenced by the *package effect* at this time but also by the pigment composition. Including all depths, $Q^*(675)$ values were (0.86, SD = 0.20) higher ($p < 0.05$) (i.e. lower *package effect*) during spring/summer than during the fall (0.73, SD = 0.19) in the Amundsen Gulf. For all depths, the high proportion of $[\text{Chl } a^{\text{Fluo}}]_{\text{pico}}$ (72 %) as well as the high averaged blue-to-red ratio (2.3, SD = 0.4) decreased throughout the fall period; both the proportion of $[\text{Chl } a^{\text{Fluo}}]_{\text{pico}}$ (62%) and the blue-to-red ratio (1.7, SD= 0.3) were low. Only the blue-to-red ratios significantly decreased ($p << 0.05$) compared to proportions of small cells ($p = 0.76$). In the Western Arctic Ocean, Matsuoka *et al.* [2011] attributed the decrease of the TChl a -specific absorption coefficient of phytoplankton during spring/summer to a strong *package effect* overwhelming the influence of the pigment composition. Under the ice cover, the average of $a_{\phi}^*(443)$ values are almost 3 times lower ($0.017 \text{ m}^2/\text{mg}$, SD = 0.005) in the Amundsen Gulf [Palmer *et al.*, 2011] than what is observed in the open water regions during our study. Thus, the increase of the cell size and *package effect* explains the increasing flattening of phytoplankton specific light absorption spectra as the open water season progresses.

As HPLC data were not available for the spring/summer period, we used the location of the absorption maxima in the red portion of the spectrum as an indicator of the presence of either green algae (Chl *b* maxima at 650 nm) or red algae (TChl *c* maxima at 635 nm) [Bricaud *et al.*, 2004]. The use of that proxy indicated that surface waters of the Amundsen Gulf were occupied by green algae (stns. 405, 2010, 1200 and 1011) and red algae (stns. 1206, 1216 and 1806). The deeper part contained a significant presence of red algae in the center and the mouth of the gulf (stns. 405, 1011, 1206 and 1806, 8010) as well as in the western side (stn. 1216). The greatest biomasses ($\langle \text{Chl } a^{\text{Fluo}} \rangle_{\text{Zeu}}$) were observed at stations 405 and 1011, corresponding to weak water stratifications ($N^2 = 0.48 - 0.51 \times 10^{-3} \text{ s}^{-2}$). The water stratification was similar ($p > 0.05$) during the spring/summer ($N^2 = 0.48 - 2.7 \times 10^{-3} \text{ s}^{-2}$) and fall ($N^2 = 0.67 - 5.5 \times 10^{-3} \text{ s}^{-2}$). The averaged biomass ($\langle \text{Chl } a^{\text{Fluo}} \rangle_{\text{Zeu}}$) was, however, three times higher during spring/summer (35 mg m^{-2}) than during fall (12 mg m^{-2}) and surprisingly, the averaged depth of SCMs was almost three times deeper (34 meters) than during the fall (13 meters). For both seasons, the concentration of Chl *a* in surface waters were similar (Table 3). This shows that the spatial division in the Amundsen Gulf between the Bank's Island coast and the upwelling region along the western coastline during fall still exists during spring/summer but the total biomass is different. As noted in section 3.2, this corresponds well to the general surface circulation pattern in that province [Lanos, 2009]. Thus, the seasonal variability of the vertical structures is important and should be considered in bio-optical models retrieving the water column-integrated phytoplankton biomass.

2.4. CONCLUSION

Our results showed that light limitation, different phytoplankton communities and cell sizes driving by physical processes are the most important sources of the observed $a_\phi^*(443)$ variability in the Canadian Arctic seas. We hypothesize that during the fall and winter, phytoplankton cells adapt to their light-limited environment by producing and grouping photosynthetic pigments (i.e. *package effect*) containing low relative concentrations of PPC. During spring and early summer, phytoplankton would have lower level of *package effect*. Adapted phytoplankton populations thus acclimate to the changing environment (i.e.

water column stratification, light and nutrient availability) by altering their cellular content and/or pigment composition. Ongoing environmental changes presently observed in the Arctic (loss of sea ice cover, increased freshwater fluxes, enhanced thermal stratification, etc.) are thus expected to further modify phytoplankton communities with yet to determine effects on the global Arctic food chain. These results are important as remote sensing of phytoplankton biomass, and ultimately primary production, in Arctic region is highly dependent on the use of accurate light absorption coefficients. Our results showed that the use of regional regressions for the retrieval of Chl *a* could improve the quantification of the phytoplankton biomass in the Canadian Arctic.

Acknowledgements

This study was supported by the Canadian IPY Federal program office, the ArcticNet Network of Canadian Centres of Excellence and the Natural Sciences and Engineering Research Council of Canada (NSERC). CBB received a scholarship from Institut des sciences de la mer de Rimouski (ISMER), stipends from Québec-Océan and financial support from Aboriginal Affairs and Northern Development Canada (AANDA) for field work. The authors want to thank the scientific team, the Canadian Coast Guard officers and the crew of the CCGS Amundsen for their help and support during the cruises, S. Roy, H. Xie, Y. Gratton, S. Ben Mustapha and M. Palmer for sampling and laboratory work, E. Alou and C. J. Mundy for technical assistance. We also thank the 2 anonymous reviewers for their constructive comments.

3. CONCLUSION

Cette étude a démontré que la limitation en lumière et en nutriments, les différents groupes phytoplanctoniques et la taille des cellules, en grande partie déterminés par les processus physiques, étaient les principales causes de la variabilité du coefficient $a_{\phi}^*(\lambda)$ dans les mers arctiques canadiennes. Les résultats soutiennent l'hypothèse qui stipule que lors de l'automne et de l'hiver, les cellules phytoplanctoniques s'adaptent à un milieu faible en intensité lumineuse, et en nutriments, en augmentant et réorganisant les pigments photosynthétiques à l'intérieur de la cellule (i.e. *effet d'empilement*) diminuant les coefficients $a_{\phi}^*(\lambda)$. À ce moment, le ratio entre les caroténoïdes photoprotecteurs et photosynthétiques (PPC:PSC) est faible. Dans le Haut-Arctique canadien, les cellules phytoplanctoniques au printemps seraient moins affectées par l'*effet d'empilement* ayant des coefficients $a_{\phi}^*(\lambda)$ significativement plus élevés et similaires aux coefficients $a_{\phi}^*(\lambda)$ mesurés dans le système de la baie d'Hudson. Les changements imminents de l'océan Arctique (diminution de l'étendue du couvert de glace l'été, augmentation des apports en eau douce et de la stratification thermale, etc.) auront donc probablement un impact considérable sur les communautés phytoplanctoniques et la chaîne alimentaire. Nos observations permettront donc d'améliorer les modèles bio-optiques et de production primaire, utilisés dans le domaine de la télédétection des eaux arctiques.

4. RÉFÉRENCES BIBLIOGRAPHIQUES

- Antoine, D., and A. Morel (1999), A multiple scattering algorithm for atmospheric correction of remotely sensed ocean colour (MERIS instrument): principle and implementation for atmospheres carrying various aerosols including absorbing ones, *Int. J. Remote Sensing*, 20(9), 1875–1916.
- Arrigo, K. R., G. V. Dijken, and S. Pabi (2008), Impact of a shrinking Arctic ice cover on marine primary production, *Geophys. Res. Lett.*, 35, L19603, doi:10.1029/2008GL035028.
- Arrigo, K. R., P. A. Matrai and G. L. van Dijken (2011), Primary productivity in the Arctic Ocean: Impacts of complex optical properties and subsurface chlorophyll maxima on large-scale estimates, *J. Geophys. Res.*, 116 (C11022), doi:10.1029/2011JC007273.
- Allali, K., A. Bricaud and H. Claustre (1997), Spatial variations in the chlorophyll-specific absorption coefficients of phytoplankton and photosynthetically active pigments in the equatorial Pacific, *J. Geophys. Res.*, 102(C6), 12, 413-12,423.
- Babin, M., J. C. Therriault, L. Legendre, and A. Condal (1993), Variations in the specific absorption coefficient for natural phytoplankton assemblages: Impact on estimates of primary production, *Limnol. Oceanogr.*, 38(1), 154–177.
- Babin, M., A. Morel, H. Claustre, A. Bricaud, Z. Kolber, and P. G. Falkowski (1996), Nitrogen- and irradiance-dependent variations of the maximum quantum yield of carbon fixation in eutrophic, mesotrophic and oligotrophic marine systems, *Deep-Sea Res. I*, 43(8), 1241–1272.

Babin, M., and D. Stramski (2002), Light absorption by aquatic particles in the near-infrared spectral region, *Limnol. Oceanogr.*, 47(3), 911–915, doi:10.1016/0967-0637(96)00058-1.

Babin, M., D. Stramski, M.G. Ferrari, H. Claustre, A. Bricaud, G. Obolensky, and N. Hoepffner (2003), Variations in the light absorption coefficients of phytoplankton, non algal particles, and dissolved organic matter in coastal waters around Europe, *J. Geophys. Res.*, 108, C73211, doi:10.1029/2001JC000882.

Barber, D. G., and M. Hanesiak (2004), Meteorological forcing of sea ice concentrations in the southern Beaufort Sea over the period 1979 to 2000, *J. Geophys. Res.*, 109, C06014, doi:10.1029/2003JC002027.

Barber, D. G., J. V. Lukovich, J. Keogak, S. Baryluk, L. Fortier, and G. H. R. Henry (2008), The changing climate of the Arctic, *Arctic*, 61, 7–26.

Bélanger, S., H. Xie, N. Krotkov, P. Larouche, W. F. Vincent, and M. Babin (2006), Photomineralization of terrigenous dissolved organic matter in Arctic coastal waters from 1979 to 2003: Interannual variability and implications of climate change, *Global Biogeochem. Cycles*, 20, GB4005, doi:10.1029/2006GB002708.

Bracher, A .U., and M. M. Tilzer (2001), Underwater light field and phytoplankton absorbance in different surface water masses of the Atlantic sector of the Southern Ocean, *Polar Biol.*, 24, 687–696.

Bricaud, A., and D. Stramski (1990), Spectral absorption coefficients of living phytoplankton and nonalgal biogenous matter: A comparison between the Peru upwelling area and the Sargasso Sea, *Limnol. Oceanogr.*, 35(3), 562–582.

Bricaud, A., M. Babin, A. Morel, and H. Claustre (1995), Variability in the chlorophyll-specific absorption coefficients of natural phytoplankton: Analysis and parameterization, *J. Geophys. Res.*, 100(C7), 13,321–13,332.

- Bricaud, A., A. Morel, M. Babin, K. Allali, and H. Claustre (1998), Variations of light absorption by suspended particles with chlorophyll *a* concentration in oceanic (case 1) waters: Analysis and implications for bio-optical models, *J. Geophys. Res.*, *103*(C13), 31,033–31,044.
- Bricaud, A., H. Claustre, J. Ras, and K. Oubelkheir (2004), Natural variability of phytoplanktonic absorption in oceanic waters: Influence of the size structure of algal populations, *J. Geophys. Res.*, *109*, C11010, doi:10.1029/2004JC002419.
- Carmack, E. C., R. W. Macdonald, and S. Jasper (2004), Phytoplankton productivity on the Canadian Shelf of the Beaufort Sea, *Mar. Ecol. Prog. Ser.*, *277*, 37–50.
- Ciotti, A. M., M. R. Lewis, and J. J. Cullen (2002), Assessment of the relationships between dominant cell size in natural phytoplankton communities and the spectral shape of the absorption coefficient, *Limnol. Oceanogr.*, *47*(2), 404–417.
- Comiso, C. J., C. L. Parkinson, R. Gersten, and L. Stock (2008), Accelerated decline in the Arctic sea ice cover, *Geophys. Res. Lett.*, *35*, L01703, doi:10.1029/2007GL031972.
- Cota, G. F., W. G. Harrison, T. Platt, S. Sathyendranath, and V. Stuart (2003), Bio-optical of the Labrador Sea, *J. Geophys. Res.*, *108*(C7), 3228–3241.
- Cota, G. F., J. Wang, and J. C. Comiso (2004), Transformation of global satellite chlorophyll retrievals with a regionally tuned algorithm, *Remote Sens. Environ.*, *90*, 373–377.
- Demers, S., S. Roy, R. Gagnon, and C. Vignault (1991), Rapid light-induced changes in cell fluorescence and xanthophylls-cycle pigments of *Alexandrium excavatum* (Dinophyceae) and *Thalassiosira pseudonana* (Bacillariophyceae): a photo-protection mechanism, *Mar. Ecol. Prog. Ser.*, *76*, 185–193.

Déry, S. J., T. J. Mlynowski, M. A. Hernández-Henríquez, and F. Straneo (2011), Interannual variability and interdecadal trends in Hudson Bay streamflow, *J. Mar. Syst.*, 88(3), 341-351.

Devred, E., C. Fuentes-Yaco, S. Sathyendranath, C. Caverhill, H. Maass, V. Stuart, T. Platt, and G. White (2005), A semi-analytic algorithm to retrieve chlorophyll- a concentration in the Northwest Atlantic Ocean from SeaWiFS data, *Indian J. Mar. Sci.*, 34(4), 356–367.

Devred, E., S. Sathyendranath, V. Stuart, Maass H., O. Ulloa, and T. Platt (2006), A two-component model of phytoplankton absorption in the open ocean: Theory and applications, *J. Geophys. Res.*, 111, C03011, doi:10.1029/2005JC002880.

Dierssen, H. M., and R. C. Smith (2000), Bio-optical properties and remote sensing ocean color algorithms for Antarctic Peninsula waters, *J. Geophys. Res.*, 105 (C11), 26,301-26,312.

Dmitriev, E. V., G. Khomenko, M. Chami, A. A. Sokolov, T. Y. Churilova, and K. K. Gennady (2009), Parameterization of light absorption by components of seawater in optically complex coastal waters of Crimea Peninsula (Black Sea), *Appl. Opt.*, 48(7), 1249–1261.

Dubinsky, Z., and N. Stambler (2009), Photoacclimation processes in phytoplankton: mechanisms, consequences, and applications, *Aquat. Microb. Ecol.*, 56, 163–176.

Falkowski, G. P., and G. T. Owens (1980), Light-shade adaptation – Two strategies in marine phytoplankton, *Plant Physiol.*, 66, 592–595.

Falkowski, P. G., Z. Dubinsky, and K. Wyman (1985), Growth-irradiance relationship in phytoplankton, *Limnol. Oceanogr.*, 30(2), 311-321.

Falkowski, P. G. and J. A. Raven (2007), Aquatic photosynthesis (second edition), Princeton University Press, Princeton.

Fargion, G. S., and J. L. Mueller (2000), *Ocean optics protocols for satellite ocean color sensor validation (revision 2)*, TM-2000-209966, NASA, Maryland.

Fofonoff, N. P., and J. R. C. Millard (1983), *Algorithms for computation of fundamental properties of seawater*, Unesco Technical Papers in Marine Science, UNESCO Publishing, Paris.

Fortier M, Fortier L, Michel C, Legendre L (2002) Climatic and biological forcing of the vertical flux of biogenic particles under seasonal Arctic sea ice. *Marine Ecology Progress Series* 225: 1-16.

Goss, R., and T. Jackob (2010), Regulation and function of xanthophylls cycle-dependent photoprotection in algea, *Photosynth. Res.*, 106, 103-122.

Granskog, M. A., R. W. Macdonald, C. J. Mundy, and D. G. Barber (2007), Distribution, characteristics and potential impacts of chromophoric dissolved organic matter (CDOM) in Hudson Strait and Hudson Bay, Canada, *Cont. Shelf Res.*, 27, 2032–2050.

Granskog, M. A., Z. Z. A. Kuzyk, K. Azetsu-Scott, and R. W. Macdonald (2011), Distributions of runoff, sea-ice melt and brine using $\delta^{18}\text{O}$ and salinity data - A new view on freshwater cycling in Hudson Bay, *J. Marine Syst.*, 88, 362-374.

Hill, V., and G. Cota (2005), Spatial patterns of primary production on the shelf, slope and basin of the Western Arctic in 2002, *Deep-Sea Res. II*, 52, 3344–3354.

Hoepffner, N., and S. Sathyendranath (1991), Effect of pigment composition on absorption properties of phytoplankton, *Mar. Ecol. Prog. Ser.*, 73, 11–23.

Hoepffner, N., and S. Sathyendranath (1992), Bio-optical characteristics of coastal waters: Absorption spectra of phytoplankton and pigment distribution in the western North Atlantic, *Limnol. Oceanogr.*, 37(8), 1660–1679.

Holmes, R. W. (1970), The Secchi disk in turbid coastal waters, *Limnol. Oceanogr.*, 15, 688–694.

Ingram, R.G., J. Bâcle, D.G. Barber, Y. Gratton, and H. Melling (2002), An overview of physical processes in the North Water, *Deep-Sea Res. II*, 49, 4893–4906.

Jeffrey, S. W., R. F. C. Mantoura, and S. W. Wright (1997), *Phytoplankton pigments in oceanography: guidelines to modern methods*, UNESCO Publishing, Paris.

Johnsen , G., and E. Sakshaug (2007), Biooptical characteristics of PSII and PSI in 33 species (13 pigment groups) of marine phytoplankton, and the relevance for pulse-amplitude-modulated and fast-repetition-rate fluorometry, *J. phycol.*, 43, 1236-1251, doi: 10.1111/j.1529-8817.2007.00422.x.

Kashino, Y., S. Kudoh, Y. Hayashi, Y. Suzuki, T. Odate, T. Hirawake, K. Satoh, M. Fukuchi (2002) Strategies of phytoplankton to perform effective photosynthesis in the North Water, *Deep-Sea Res. II*, 49, 5049 – 5061.

Kashino, Y., and S. Kudoh (2003), Concerted response of xanthophylls-cycle pigment in a marine diatom, *Chaetoceros gracilis*, to shifts in light condition, *Phycol. Res.*, 51, 168–172.

Kirk, J. T. O. (1994), *Light and photosynthesis in aquatic ecosystems, second edition*, Cambridge University Press, Cambridge.

Kishino, M., M. Takahashi, N. Okami, and S. Ichimura (1985), Estimation of the spectral absorption coefficients of phytoplankton in the sea, *Bull. Mar. Sci.*, 37(2), 634-642.

- Klein, B., B. LeBlanc, Z. P. Mei, R. Beret, J. Michaud, C.J. Mundy, C. H. Quillfeldt, M. È. Garneau, S. Roy, Y. Gratton, J. K. Cochran, S. Bélanger, P. Larouche, J. D. Pakulski, R. B. Rivkin, and L. Legendre (2002), Phytoplankton biomass, production and potential export in the North Water, *Deep-Sea Res. II*, **49**, 4983–5002.
- Lammers, R. B., A. I. Shikloman, C. J. Vorusmarty, B. M . Fekete and B. J. Peterson (2001), Assessment of contemporary Arctic river runoff based on observational discharge records, *J. Geophys. Res.*, **106** (D4), 3321-3334.
- Lanos, R. (2009), Circulation régionale, masses d'eau, cycles d'évolution et transports entre la mer de Beaufort et le Golfe d'Amundsen, PhD thesis, Université du Québec, Canada, 245 pp.
- Lapoussière A, Michel C, Gosselin M, Poulin M (2009) Spatial variability in organic material sinking export in the Hudson Bay system, Canada, during fall. *Continental Shelf Research* **29**: 1276-1288.
- Lavaud, J., B. Rousseau, and A.-L. Etienne (2004), General features of photoprotection by energy dissipation in planktonic diatoms (bacillariophyceae), *J. phycol.*, **40**, 130-137.
- Lovejoy, C., L. Legendre, M. J. Martineau, J. Bâcle, and C. H. Quillfeldt (2002), Distribution of phytoplankton and other protists in the North Water, *Deep-Sea Res. II*, **49**, 5027–5047.
- Lovejoy, C., W. F. Vincent, S. Bonilla, S. Roy, M.-J. Martineau, R. Terrado, M. Potvin, R. Massana, and C. Pedrós-Alió (2007), Distribution, phylogeny, and growth of cold-adapted picoprasinophytes in arctic seas, *J. Phycol.*, **43**, 78–89.
- Lund J.W.G., C. Kipling and E. D. Le Cren (1958), *The Inverted Microscope Method of Estimating Algal Numbers and the Statistical Basis of Estimations by Counting*, Freshwater Biological Association, The Ferry House, Ambleside, Westmorland, England.

Lutz, V. A., S. Sathyendranath, E. J. H. Head, and W. K. W. Li (2003), Variability in pigment composition and optical characteristics of phytoplankton in the Labrador Sea and the central North Atlantic, *Mar. Ecol. Prog. Ser.*, 260, 1–18.

Macdonald, R. W., T. Harner, and J. Fyfe (2005), Recent climate change in the Arctic and its impact on contaminant pathways and interpretation of temporal trend data, *Sci. Total Environ.*, 342, 5–86.

Martin, J., J. É. Tremblay, J. Gagnon, G. Tremblay, A. Lapoussiére, C. Jose, M. Poulin, M. Gosselin, Y. Gratton, and C. Michel (2010), Prevalence, structure and properties of subsurface chlorophyll maxima in Canadian Arctic waters, *Mar. Ecol. Prog. Ser.*, 412, 69–84.

Matsuoka, A., Y. Huot, K. Shimada, S. I. Saitoh, and M. Babin (2007), Bio-optical characteristics of the western Arctic Ocean: implications for ocean color algorithms, *Can. J. Remote Sensing*, 33(6), 503–518.

Matsuoka, A., P. Larouche, M. Poulin, W. Vincent, and H. Hattori (2009), Phytoplankton community adaptation to changing light levels in the southern Beaufort Sea, Canadian Arctic, *Estuar., Coast. Shelf Sci.*, 82, 537–546.

Matsuoka, A., V. Hill, Y. Huot, M. Babin, and A. Bricaud (2011), Seasonal variability in the light absorption properties of western Arctic waters: Parameterization of the individual components of absorption for ocean color applications, *J. Geophys. Res.*, 116, C02007, doi:10.1029/2009JC005594.

Melling, H., Y. Gratton Y, and G. Ingram (2001), Ocean circulation within the North Water Polynya of Baffin Bay, *Atmos. Ocean*, 39(3), 301–325.

Mitchell, B. G. (1990), Algorithms for determining the absorption coefficient of aquatic particulates using the quantitative filter technique (QFT), *Ocean Optics X*, 137–148.

Morel, A. and A. Bricaud (1981) Theoretical results concerning light absorption in a discrete medium, and application to specific absorption of phytoplankton, *Deep-Sea Res.*, 28A(11), 1393-1981.

Morel, A., and Y.-H. Ahn (1990), Optical efficiency factors of free-living marine bacteria: Influence of bacterioplankton upon the optical properties and particulate organic carbon in oceanic waters, *J. Mar. Res.*, 48, 145-175.

Morel, A. (1991), Optics of marine particles and marine optics, *Part. Analysis Oceanogr.*, G27, 141-188.

Moreno, D. V., J. P. Marrero, J. Morales, C. L. García, M. G. V. Úbeda, M.J. Rueda and O. Llinás (2012), Phytoplankton functional community structure in Argentinian continental shelf determined by HPLC pigment signatures, *Estuar., Coast. Shelf Sci.*, 100, 72-81.

O'Reilly, J. E., S. Maritorena, B. G. Mitchell, D. A. Siegel, K. L. Carder, S. A. Garver, M. Kahru, and C. McClain (1998), Ocean color chlorophyll algorithms for SeaWiFS, *J. Geophys. Res.*, 103(C11), 24,937-24,953.

O'Reilly, J. E., S. Maritorena, D. A. Siegel, M. C. O'Brien, D. Toole, B. G. Mitchell, M. Kahru, F. P. Chavez, P. Strutton, G. F. Cota, S.B. Hooker, C. R. McClain, K. L. Carder, F. Muller-Karger, L. Harding, A. Magnuson, D. Phinney, G. F. Moore, J. Aiken, K. R. Arrigo, R. Letelier, and M. Culver (2000), Ocean color chlorophyll *a* algorithms for SeaWiFS: Version 4, SeaWiFS Postlaunch Calibration and Validation Analyses, Part 3, NASA Technical Memorandum 2000-206892, Vol. 11, NASA, Goddard Space Flight Center, Greenbelt, Maryland.

Pabi, S., G. L. van Dijken and K. R. Arrigo (2008), Primary production in the Arctic Ocean, 1998–2006, *J. Geophys. Res.*, 113(C08005), doi:10.1029/2007JC004578.

Palmer, A. Molly, K. R. Arrigo, C. J. Mundy, J. K. Ehn, M. Gosselin, D. G. Barber, J. Martin, E. Alou, S. Roy, J. É. Tremblay (2011), Spatial and temporal variation of photosynthetic parameters in natural phytoplankton assemblages in the Beaufort Sea, Canadian Arctic (2011) , *Polar Biol.*, 34, 1915–1928, doi: 10.1007/s00300-011-1050-x.

Parsons, T. R., Y. Maita, and C. M. Lalli (1984), *A manual of chemical and biological methods for seawater analysis*, Pergamon Press, Toronto.

Pegau, W. S. (2002), Inherent optical properties of the central Arctic surface waters, *J. Geophys. Res.*, 107(C10), doi:10.1029/2000JC000382.

Pond, S., and G. L. Pickard (2005), *Introductory dynamic oceanography, second edition*, Pergamon Press, Oxford, England.

Retamal, L., W. F. Vincent, C. Martineau, and L. Osburn (2007), Comparison of the optical properties of dissolved organic matter in two river-influenced coastal regions of the Canadian Arctic, *Estuar. Coast. Shelf Sci.*, 72, 261–272.

Retamal, L., S. Bonilla, and W. F. Vincent (2008), Optical gradients and phytoplankton production in the Mackenzie River and the coastal Beaufort Sea, *Polar Biol.*, 31, 363–379, doi:10.1007/s00300-007-0365-0.

Reynolds, R. A., D. Stramski, and B. G. Mitchell (2001), A chlorophyll-dependent semi-analytical reflectance model derived from field measurements of absorption and backscattering coefficients within the Southern Ocean, *J. Geophys. Res.*, 106 (C4), 7125–7138.

Roy, S., F. Blouin, A. Jacques, and J. C. Therriault (2008), Absorption properties of phytoplankton in the lower Estuary and Gulf of St. Lawrence (Canada), *Can. J. Fish. Aquat. Sci.*, 65, 1721–1737.

Sathyendranath, S., G. Cota, V. Stuart, H. Maass, and T. Platt (2001), Remote sensing of phytoplankton pigments: A comparison of empirical and theoretical approaches, *Int. J. Remote Sens.*, 22(2-3), 249–273.

Sathyendranath, S., L. Watts, E. Devred, T. Platt, C. Caverhill, and H. Maass (2004), Discrimination of diatoms from other phytoplankton using ocean-colour data, *Mar. Ecol. Prog. Ser.*, 272, 59–68.

Stramska, M., and D. Stramski (2003) Bio-optical relationships and ocean color algorithms for the north polar region of the Atlantic, *J. Geophys. Res.*, 108(C5), doi:10.1029/2001JC001195.

Tassan, S., and G. M. Ferrari (2002), A sensitivity analysis of the ‘Transmittance-Reflectance’ method for measuring light absorption by aquatic particles, *J. Plankton Res.*, 24(8), 757–774.

Tremblay, J. É., Y. Gratton, J. Fauchot, and N. M. Price (2002), Climatic and oceanic forcing of new, net, and diatom production in the North Water, *Deep-Sea Res. II*, 49, 4927–4946.

Tremblay, J. É., H. Hattori, C. Michel, M. Ringuette, Z. P. Mei, C. Lovejoy, L. Fortier, K. A. Hobson, D. Amiel, and K. Cochran (2006), Trophic structure and pathways of biogenic carbon flow in the eastern North Water Polynya, *Prog. Oceanogr.*, 71, 402–425.

Tremblay, J. É., K. Simpson, J. Martin, L. Miller, Y. Gratton, D. Barber, and N. M. Price (2008), Vertical stability and the annual dynamics of nutrients and chlorophyll fluorescence in the coastal, southern Beaufort Sea, *J. Geophys. Res.*, 113(C07S90), doi:10.1029/2007JC004547.

Tremblay, G., C. Belzile, M. Gosselin, M. Poulin, S. Roy, and J.É. Tremblay (2009), Late summer phytoplankton distribution along a 3500 km transect in Canadian Arctic waters: strong numerical dominance by picoeukaryotes, *Aquat. Microb. Ecol.*, 54, 55–70.

Uitz, J., H. Claustre, A. Morel, and S. B. Hooker (2006), Vertical distribution of phytoplankton communities in open ocean: An assessment based on surface chlorophyll, *J. Geophys. Res.*, 111, C08005, doi:10.1029/2005JC003207.

Vidussi, F., H. Claustre, B. B. Manca, A. Luchetta, and J. C. Marty (2001), Phytoplankton pigment distribution in relation to upper thermocline circulation in the eastern Mediterranean, *J. Geophys. Res.*, 106, 19,939–19,956.

Vidussi, F., S. Roy, C. Lovejoy, M. Gammelgaard, H.A. Thomsen, B. Booth, J. É. Tremblay, and B. Mostajir (2004), Spatial and temporal variability of the phytoplankton community structure in the North Water Polynya, investigated using pigment biomarkers, *Can. J. Fish. Aquat. Sci.*, 61(11), 2038–2052.

Wang, J., and G. F. Cota (2003), Remote sensing reflectance in the Beaufort and Chukchi seas: observations and models, *Appl. Opt.*, 42(15): 2754–2765.

Wang, J., G. F. Cota, and D. A. Ruble (2005), Absorption and backscattering in the Beaufort and Chukchi Seas, *J. Geophys. Res.*, 110, C04014, doi:10.1029/2002JC001653.

Zapata, M., and R. F. Garrido (2000), Separation of chlorophylls and carotenoids from marine phytoplankton: a new HPLC method using a reversed phase C₈ column and pyridine-containing mobile phases, *Mar. Ecol. Prog. Ser.*, 195, 29–45.

